Ricardo Claudino

Insights into Polyhydroxyalkanoates (PHAs) in Extremophile Microorganisms: Search for PHA-related genes and PHA accumulation in members of the genus *Rubrobacter*

UAlg
UNIVERSIDADE DO ALGARVE

Faculty of Science and Technology

2022-2023

Ricardo Claudino

Insights into Polyhydroxyalkanoates (PHAs) in Extremophile Microorganisms: Search for PHA-related genes and PHA accumulation in members of the genus *Rubrobacter*

Thesis for master's degree in Biotechnology

Under the supervision of:

Conceição Egas, Ph.D.

University of Coimbra | Center for Neuroscience and Cell Biology

Cantanhede, Portugal

&

Helena Maria Leitão Demigné Galvão, Ph.D.

University of Algarve | Center for Marine and Environmental Research

Faro, Portugal

Faculty of Science and Technology

2022-2023

Insights into Polyhydroxyalkanoates (PHAs) in Extremophile Microorganisms: Search for PHA-related genes and PHA accumulation in members of the genus *Rubrobacter*

Declaração de autoria de trabalho

Declaro ser o autor deste trabalho, que é original e inédito. Autores e trabalhos consultados estão devidamente citados no texto e constam da listagem de referências incluída.

Universidade do Algarve, Setembro 2023

_____

(Ricardo Claudino)

"The only true wisdom is in knowing you know nothing."

- Socrates

Index

Acknowledgments I
Abbreviations and acronyms II
Index of figures IV
Index of tables VI
Abstract VII
Resumo IX
1. Introduction 1
1.1. Framework - Today's plastic problem 1
1.2. Alternative use of plastics – Bioplastics 2
1.3. Polyhydroxyalkanoate 3
1.3.1. PHA overview 3
1.3.2. PHA classifications and main characteristics 5
1.3.3. PHA synthase classification 6
1.3.4. PHA biosynthesis and major metabolic pathway 7
1.3.5. Accumulation of PHA in microorganisms 9
1.3.6. Fermentation methods and strategies for PHA production 10
1.3.6.1. Fed-batch culture 10
1.3.6.2. Batch culture 11
1.3.6.3. Continuous culture 11
1.3.7. Extraction of PHA 11
1.3.7.1. Chemical extraction 12
1.3.7.2. Mechanical extraction 12
1.3.7.3. Enzymatic extraction 12
1.3.7.4. Supercritical fluid extraction 13
1.3.7.5. Sonication extraction 13
1.3.8. PHA detection, characterization and quantification methods 13
1.3.9. Biodegradation of PHA 16
1.3.10. PHA biotechnological applications and current trends 17
1.3.11. PHA role in extremophile species 18
1.4. The genus *Rubrobacter* 19
1.4.1. Relationship between *Rubrobacter* species and PHA accumulation 20
1.5. Objectives 21
2. Materials and methods 23
2.1. Microorganism selection 23
2.2. *In silico* analysis of genes involved in PHA synthesis 23
2.3. Growth media 24

2.3.1. Culture conditions optimization 24
2.3.2. Growth media for biomass production 24
2.3.3. Growth media for enhanced PHA accumulation 26
2.4. Staining techniques 27
2.4.1. Plate assay 27
2.4.2. Sudan black staining 28
2.5. Microscope analysis 28
2.5.1. Optical microscopy visualization of the PHA granules 28
2.5.2. Transmission electron microscopy 28
2.6. PHA extraction and detection technique 29
2.6.1. Halogenated solvent PHA extraction 29
2.6.2. PHA detection 30
3. Results 31
3.1. Identification of PHA-related genes in the *Rubrobacter* genus 31
3.1.1. PhaA 31
3.1.2. PhaB 32
3.1.3. PHA synthase 33
3.1.3.1. Lipase box-like in phaC 34
3.2. Phenotypic analysis 36
3.2.1. Growth media conditions optimization 36
3.2.2. Biomass production 38
3.2.3. Enhanced PHA accumulation 40
3.2.4. Plate assay method for rapid detection of PHA accumulators 40
3.2.5. Sudan black staining and optical microscopy 41
3.2.6. Transmission electron microscopy 43
3.2.7. Detection of PHA 44
4. Discussion....47
5. Conclusion and future work 55
6. Bibliography 57
7. Annexes 69

Acknowledgments

First of all, I would like to express my sincere gratitude to my supervisor, Conceição Egas. She was always available and ready to offer guidance and knowledge through their mentorship. I am profoundly thankful for all the lessons she gave during this journey.

Furthermore, I extend my deepest gratitude to my other supervisor, Helena Galvão, for graciously accepting my invitation to join me on this academic journey.

I am also indebted to my course supervisor, Deborah Power. Her constant willingness to help has been fundamental to my academic growth.

I'd also like to say a huge thank you to Luciana for helping with everything I needed in the laboratory.

My sincere thanks go to all my colleagues at the CNC, who have been a pillar of support throughout this project. Together, we have faced challenges and shared moments of laughter, creating a fun atmosphere.

To my dear family, whose unconditional love and support have been the foundation of my journey. Mom and Dad, your efforts to secure my future have not gone unnoticed and I am deeply grateful for your sacrifices!

Finally, I would like to thank the incredible friends who stood by me when I needed them most. Special thanks to David Sales, Ana Santos and Mariana Galvan who were my best friends during the difficult times!

Abbreviations and acronyms

BLAST - basic local alignment search tool

CDW - cellular dry weight

CNC - Center for Neuroscience and Cell Biology

EU - European Union

FT-IR - fourier transform-infrared spectroscopy

GC-MS - gas chromatography-mass spectrometry

HAs - (R)-3-hydroxy fatty acids monomers

HPLC - high-performance liquid chromatography

ICBAS - Instituto de Ciências Biomédicas Abel Salazar

ICNP - International Code of Nomenclature of Prokaryotes

kHz - kilohertz

lcl-PHAs - long-chain length PHAs

mcl-PHAs - medium-chain length PHAs

MSM - mineral salt medium

NCBI - National Center for Biotechnology Information

NTA - nitrilotriacetic acid

P(3HB) - poly-3-hydroxybutyrate

P(3HB-co-3HV) - poly(3-hydroxybutyrate-co-3-hydroxyvalerate)

P(3HB-co-3MP) - poly(3-hydroxybutyrate-co-3-mercaptopropionate)

P(3HHx-co-3HO) - poly(3-hydroxyhexanoate-co-3-hydroxyoctanoate)

P(3HV) - poly-3-hydroxyvalerate

P4HB - poly-4-hydroxybutyrate

PBAT - polybutylene adipate terephthalate

PBS - polybutylene succinate

PE - polyethylene

PEF - polyethylene furanoate

PET - polyethylene terephthalate

PHA(s) – polyhydroxyalkanoate(s)

phaA - beta-ketothiolase

phaB - NAD(P)H-dependent acetoacetyl-CoA reductases

phaC - PHA synthase

phaE - class III specific PHA synthase subunit

phaR - class IV specific PHA synthase subunit

phaZ - PHA depolymerase

PHB – polyhydroxybutyrate

PHBHHx - poly(3-hydroxybutyrate-co-3-hydroxyhexanoate)

PHBV - poly(3-hydroxybutyrate-co-3-hydroxyvalerate)

PHP - poly-3-hydroxypropionate

PHPV - poly(3-hydroxy-5-phenyl-valerate)

PLA - polylactic acid

PP - polypropylene

PTT - polytrimethylene terephthalate

R - alkyl side chain

scl-PHAs - short-chain length PHAs

SEM - scanning electron microscopy

TEM – transmission electron microscopy

UV – ultraviolet

UV-Vis - UV-visible spectroscopy

W - watts

Index of figures

Figure 1.1. - Price trends, in American dollars, for Brent crude oil barrels, between 2020 and early 2023. Adapted from King (2023). 2

Figure 1.2. - Various conventional plastics and bioplastic materials such as polyethylene (PE), polypropylene (PP), polyethylene terephthalate (PET), polytrimethylene terephthalate (PTT), polyethylene furanoate (PEF), polybutylene adipate terephthalate (PBAT), polycaprolactone (PCL), polylactic acid (PLA), polybutylene succinate (PBS) and polyhydroxyalkanoate (PHA), with varying qualities based on origin and biodegradability. Adapted from Fredi and Dorigato (2021).....3

Figure 1.3. - PHA basic structure. R: Type of alkyl side chain. X: Number of methylene groups in the monomer backbone. n: number of polymer chain's repeating units. Adapted from Możejko-Ciesielska and Kiewisz (2016). 5

Figure 1.4. - Some selected examples of PHA, according to how many carbon atoms make up each monomer unit. Poly-3-hydroxybutyrate (P(3HB)), poly-3-hydroxypropionate (PHP), poly-4-hydroxybutyrate (P4HB) and poly-3-hydroxyvalerate (P(3HV)) are represented as scl-PHAs. poly(3-hydroxybutyrate-co-3-hydroxyvalerate) (PHBV) and poly(3-hydroxybutyrate-co-3-hydroxyhexanoate) (PHBHHx) are represented as mcl-PHAs. Adapted from Kaniuk and Stachewicz (2021). 6

Figure 1.5. - The main metabolic pathway for the P(3HB) synthesis, the most synthesized PHA globally. phaA: beta-ketothiolase. phaB: NAD(P)H-dependent acetoacetyl-CoA reductases. phaC: PHA synthase. phaZ: PHA depolymerase. Adapted from Alcântara et al. (2020).....8

Figure 3.1. - Partial sequence alignment of the *phaC* encoded protein with the corresponding lipase box-like conserved region. A: phaC class I PHA synthetase subunit. B: phaC class III PHA synthetase subunit. All the sequences are related to the selected *Rubrobacter* species with reported phaC synthase subunit. The sequences were retrieved from the GenBank public database and aligned with the Clustal Omega tool within the MEGA11 software and visualized with the Espript 3.0. online tool. 36

Figure 3.2. - *R. xylanophilus* DSM 9941^T and *R. radiotolerans* DSM 5868^T growth curves. TN: *Thermus* medium (tryptone and yeast extract concentrations of 1 g/L). T2.5: *Thermus* medium (tryptone and yeast extract concentrations of 2.5 g/L). T5: *Thermus* medium (tryptone and yeast extract concentrations of 5 g/L). TSB: Tryptic soy broth..38

Figure 3.3. - Growth curves at the optimum growth temperature in *Thermus* medium. 1: *R. bracarensis* CECT 7924^T. 2: *R. aplysinae* CECT 8425^T. 3: *R. radiotolerans* DSM 5868^T. 4: *R. radiotolerans* RSPS-4. 293^T. 5: *R. xylanophilus* DSM 9941^T. 6: *R. calidifluminis* RG-1^T. 7: *R. naiadicus* RG-3^T. 8: *R. taiwanensis* LS-293^T. 39

Figure 3.4. - *Rubrobacter* species growth curve in MSM supplemented with 2% glucose. 1: *R. radiotolerans* DSM 5868^T. 2: *R. radiotolerans* RSPS-4. 3: *R. xylanophilus* DSM 9941^T. 4: *R. calidifluminis* RG-1^T. 5: *R. naiadicus* RG-3^T. 6: *R. taiwanensis* LS-293^T. 40

Figure 3.5. - Plate assay method for PHA production detection. A: RR: *R. radiotolerans* RSPS-4. Control - E. coli: *E. coli* ATCC 29922. B: RX: *R. xylanophilus* DSM 9941^{T}. RN: *R. naiadicus* RG-3^{T}. RC: *R. calidifluminis* RG-1^{T}. 41

Figure 3.6. - *Rubrobacter* species selected for observation using the Sudan black B staining technique under an optical microscope (Carl Zeiss Axio Imager A2) with a 100x oil immersion objective. A: *R. xylanophilus* DSM 9941^{T}. B: *R. radiotolerans* RSPS-4. C: *R. radiotolerans* DSM 5868^{T}. D: *R. calidifluminis* RG-1^{T}. E: *R. naiadicus* RG-3^{T}. F: *R. taiwanensis* LS-293^{T}. G: *R. bracarensis* CECT 7924^{T}. H: *R. aplysinae* CECT 8425^{T}. A, B, C, D, E and F grown during 48 hours in MSM. G and H grown during 120 hours in *Thermus* medium. 42

Figure 3.7. - *Rubrobacter* species selected for TEM observation. A: *R. xylanophilus* DSM 9941^{T}. B: *R. radiotolerans* RSPS-4. C: *R. radiotolerans* DSM 5868^{T}. D: *R. taiwanensis* LS-293^{T}. Cells were observed after cultivation in MSM, for 24 hours, at their optimal growth temperature. 44

Figure 3.8. - Measurement of crotonic acid by absorbance between 200 nm and 260 nm of *Rubrobacter* species. 1: *R. xylanophilus* DSM 9941^{T}. 2: *R. radiotolerans* DSM 5868^{T}, 3: *R. radiotolerans* RSPS-4. 4: *R. taiwanensis* LS-293^{T}. 5: *R. calidifluminis* RG-1^{T}. 6: *R. naiadicus* RG-3^{T}. 7: *R. bracarensis* CECT 7924^{T}. 8: *R. aplysinae* CECT 8425^{T}. 9: *E. coli* ATCC 29922. 1, 2, 3, 4, 5 and 6 grown during 48 hours in MSM. 7 and 8 grown during 120 hours in *Thermus* medium. 9 grown during 24 hours in LB medium. 45

Figure 7.1. - Full sequence alignment of the *phaC* encoded protein class I.....70

Figure 7.2. - Full sequence alignment of the *phaC* encoded protein class III 72

Index of tables

Table 2.1. A - *Thermus* medium, pH 7.0 (Carreto et al., 1996). 25

Table 2.1. B - *Thermus* medium concentrated solutions 26

Table 2.2. - Tryptic soy broth medium (DIFCO), pH 7.0 26

Table 2.3. - MSM, pH 7.0 (Kouřilová et al., 2021). 27

Table 3.1. – Similarity and comparison between the phaA amino acid sequence of *R. xylanophilus* DSM 9941^T and the phaA amino acid sequences found in other selected *Rubrobacter* species. The information was retrieved from the GenBank public database. 32

Table 3.2. - Similarity and comparison between the phaB amino acid sequence of *R. xylanophilus* DSM 9941^T and the phaB amino acid sequences found in other selected *Rubrobacter* species. The information was retrieved from the GenBank public database. 33

Table 3.3. - PHA synthases (class I and class III) along with their constituent subunits, examined in the selected *Rubrobacter* species. The information was retrieved from the GenBank public database. 34

Table 4.1. - Summary table of experimental results. 48

Abstract

This thesis investigates the potential of polyhydroxyalkanoates (PHAs) production by extremophile microorganisms. PHA offers advantages over conventional fossil-fuel-based plastics due to their biodegradability and bio-based origin. Among extremophiles capable of producing PHA, species of the genus *Rubrobacter* are promising contenders and were chosen for this investigation. The research involved a bioinformatic analysis of *Rubrobacter* genomes, specifically examining the presence of key genes (*phaA*, *phaB*, *phaC*) belonging to the PHA synthesis pathway. Since only some of the species studied possess the class I PHA synthase, suggested potential differences in PHA synthesis capabilities. Further investigation into the phaC lipase box-like motif, pointed to variations in their conserved region which may also impact the capacity of PHA synthesis by different *Rubrobacter* species. The synthesis of PHA was then tested experimentally. *Thermus* medium emerged as the most suitable to grow the organisms and to standardize experimental conditions. Potentiation of PHA accumulation was achieved in a minimal medium supplemented with glucose as a carbon source. With the Sudan Black B method, it was possible to identify the *Rubrobacter xylanophilus* DSM 9941^{T}, *Rubrobacter radiotolerans* RSPS-4 and *Rubrobacter radiotolerans* DSM 5868^{T} species as PHA accumulators. Confirmation of PHA accumulation was achieved through transmission electron microscopy and an indirect PHA detection method. Notably, the presence of the class I PHA synthases in the studied species correlated with successful PHA production, emphasizing its significance and concluding an identification of a link between genomic characteristics and phenotypic outcomes in PHA synthesis within the thermophilic *Rubrobacter* species studied. Future research should include exploring the specific types of PHA produced by different species and assessing economic viability based on production costs and market demand, which is crucial for commercial use.

Keywords: Polyhydroxyalkanoates (PHAs); Extremophiles; *Rubrobacter*; Thermophilic; Bioinformatics analysis; Phenotypic analysis; PHA synthesis

Resumo

Esta tese investiga o potencial de produção de polihidroxialcanoatos (PHAs) por microrganismos extremófilos. O PHA oferece vantagens sobre os plásticos convencionais à base de combustíveis fósseis devido à sua biodegradabilidade e origem biológica. Entre os extremófilos capazes de produzir PHA, as espécies do género *Rubrobacter* são candidatos promissores e foram escolhidas para esta investigação. A investigação envolveu uma análise bioinformática dos genomas de *Rubrobacter*, examinando especificamente a presença dos genes-chave (*phaA*, *phaB*, *phaC*) pertencentes à via metabólica de PHA. Uma vez que apenas algumas das espécies estudadas possuem a PHA sintase da classe I, este facto sugere potenciais diferenças nas capacidades de síntese de PHA. Uma pesquisa mais aprofundada na região phaC "*lipase box-like motif*" apontou também para variações na região conservada, que também podem afetar a capacidade de síntese de PHA nas diferentes espécies de *Rubrobacter*. A síntese de PHA foi então testada experimentalmente. O meio *Thermus* destacou-se como o mais adequado para cultivar os organismos e padronizar as condições experimentais. A potenciação da acumulação de PHA foi alcançada num meio mínimo suplementado com glucose como fonte de carbono. Com o método do Sudan Black B, foi possível identificar as espécies *Rubrobacter xylanophilus* DSM 9941^{T}, *Rubrobacter radiotolerans* RSPS-4 e *Rubrobacter radiotolerans* DSM 5868^{T} como acumuladores de PHA. A confirmação da acumulação de PHA foi obtida através de microscopia eletrónica de transmissão e de um método de deteção indireta de PHA. Notavelmente, a presença da PHA sintase da classe I nas espécies estudadas correlacionou-se com a produção bem-sucedida de PHA, enfatizando a sua importância e concluindo a identificação de uma ligação entre as características genómicas e os resultados fenotípicos na síntese de PHA dentro das espécies termofílicas de *Rubrobacter* estudadas. Pesquisas futuras devem incluir a exploração dos tipos específicos de PHA produzidos por pelas diferentes espécies e a avaliação da viabilidade económica com base nos custos de produção e na procura de mercado, o que é crucial para a sua utilização comercial.

Palavras-chave: Polihidroxialcanoatos (PHAs); Extremófilos; *Rubrobacter*; Termofílicas; Análise bioinformática; Análise fenotípica; Síntese de PHA

1. Introduction

1.1 Framework - Today's plastic problem

Synthetic plastics have transformed society since the 20th century thanks to their fascinating aspects, such as lightness and durability, qualities attributed to a low-cost material and replacing others with higher manufacturing costs, such as paper, glass and metals (Thakur et al., 2018). However, the properties of the current plastics that everyone uses, day after day, damage the environment, as it does not degrade fast enough, snowballing the complications of this commodity (Chamas et al., 2020). Even the production of plastics is a significant source of environmental pollution, leading to the contamination of seas and rivers due to the release of minuscule waste particles from manufacturing facilities (Kasavan et al., 2021).

Because of this, governments and individuals are starting to think more critically about the effects of industrial waste and personal consumption. Some progress is already being made by reducing the use of single-use plastics. One of the countries that implemented this measure was Portugal, starting on the 1 of July 2021, in several steps, dictated by the European Union (EU) directives regarding this subject, where the first step was forbidding any distribution of free bags in supermarkets or equivalent, due to being one of the most littered objects in the EU. As an alternative, the use of paper or plastic bags from more sustainable sources was introduced, with a small fee, to encourage the reuse of these environmentally friendly options (Prata et al., 2022).

The events of 2022 drove up oil prices, which had been growing sharply over the previous years, to all-time highs (Figure 1.1.). Although, at the time of writing this thesis, the price of oil has decreased and stabilized, this does not guarantee that it may not increase again due to other external factors, as numerous variables, including new geopolitical developments and natural disasters, have a significant impact on the oil market and consequently, on the cost of plastic manufacture (Bagchi & Paul, 2023; Onour & Abdo, 2022).

Thus, in addition to the environmental impacts that current plastic produces, the economic factor is also increasingly unfavorable to its production, with more environmentally friendly alternatives emerging exponentially as the best option, such as bioplastics (Appiah-Otoo, 2022; Prata et al., 2022).

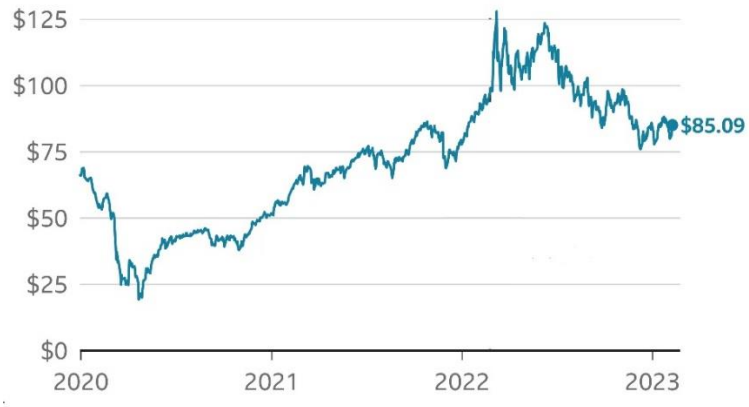

Figure 1.1. - Price trends, in American dollars, for Brent crude oil barrels, between 2020 and early 2023. Adapted from King (2023).

1.2. Alternative use of plastics – Bioplastics

In recent years, the plastic industry has begun to move away from fossil fuel-based plastics and has started to produce bioplastics by manufacturing polymers from renewable resources. Due to the growing popularity of bioplastics, there is often a lack of clarity in their definition, as the term is frequently used to encompass various materials with different characteristics. For instance, it is common to include bio-based or biodegradable plastics under the umbrella of bioplastics, which can lead to confusion and misinterpretation (Figure 1.2.) (Ibrahim et al., 2021).

To clarify, it should be noted that bio-based plastics are manufactured using sustainably sourced materials or biomass, partially or entirely, but it is not granted that these bio-based plastics are biodegradable. Some examples of bio-based, non-biodegradable bioplastics include bio-based polyethylene (PE), polypropylene (PP), polyethylene terephthalate (PET), polytrimethylene terephthalate (PTT) and polyethylene furanoate (PEF) (Siracusa & Blanco, 2020).

On the other hand, biodegradable bioplastics can be disintegrated into smaller, monomeric compounds and are processed and decomposed by microorganisms, usually in a composter, bioreactor or outdoors, within an appropriate location (Kjeldsen et al., 2018). However, this does not mean that biodegradable bioplastic is necessarily made from sustainable materials or production. Polybutylene adipate terephthalate (PBAT) is an example of a biodegradable, non-bio-based bioplastic (Jian et al., 2020).

The most important thing here is what they are intended for and what it is aimed for is biobased bioplastics with biodegradable capability, where the most crucial factor is to reduce the ecological footprint (Atiwesh et al., 2021). Recent developments have made it possible to employ, on a commercial level, some promising polymers, such as polylactic acid (PLA), polybutylene succinate (PBS) and polyhydroxyalkanoates (PHAs), as a bio-based, biodegradable replacement, in several applications that currently use petroleum-based and non-biodegradable plastics (Meereboer et al., 2020; Siracusa & Blanco, 2020).

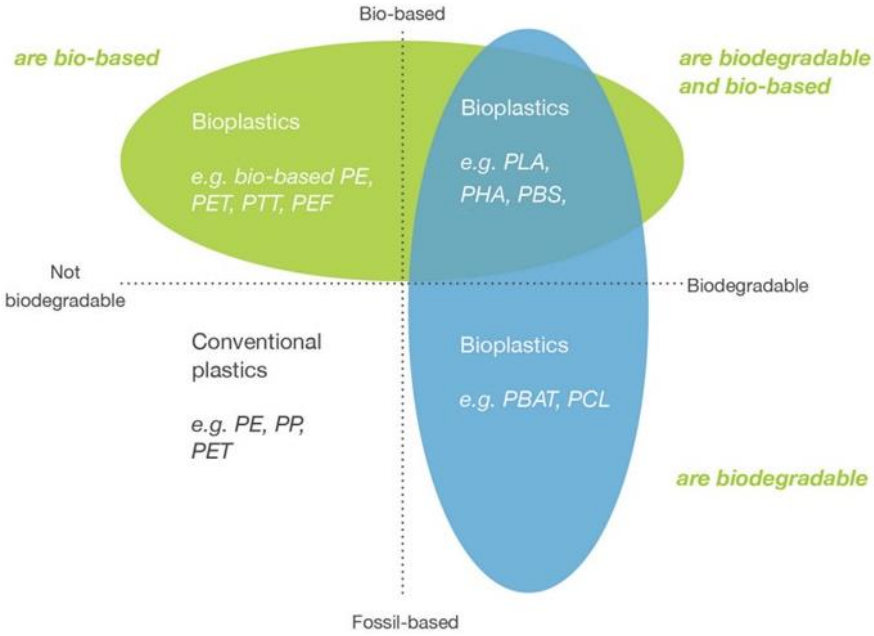

Figure 1.2. - Various conventional plastics and bioplastic materials such as polyethylene (PE), polypropylene (PP), polyethylene terephthalate (PET), polytrimethylene terephthalate (PTT), polyethylene furanoate (PEF), polybutylene adipate terephthalate (PBAT), polycaprolactone (PCL), polylactic acid (PLA), polybutylene succinate (PBS) and polyhydroxyalkanoate (PHA), with varying qualities based on origin and biodegradability. Adapted from Fredi and Dorigato (2021).

1.3. Polyhydroxyalkanoate

1.3.1. PHA overview

Polyhydroxyalkanoate (PHA), is a polyester composed of (R)-3-hydroxy fatty acids monomers (HAs), which is synthesized by several bacteria and archaea (Możejko-Ciesielska & Kiewisz, 2016). It has the unique characteristic of biodegrading completely under both aerobic and anaerobic conditions without leaving any harmful chemical residues (Tokiwa et al., 2009). As said previously, PHAs can be processed and used for bioplastics manufacture, substituting fossil fuel-derived polymers (Możejko-Ciesielska

& Kiewisz, 2016). Because of that, it is established as a highly promising polymer for scientific exploration and widespread commercial applications (Meereboer et al., 2020).

The first time PHAs were observed was in 1888, by the Dutch microbiologist Martinus Willem Beijerinck, who detected intracellular inclusions that were described as a type of lipids (Palmeiro-Sánchez et al., 2022). However, it was the French researcher Maurice Lemoigne, in 1926, who first succeeded in accurately identifying PHA granules and described them as a polyhydroxybutyrate (PHB) homopolymer, one of the members of the PHA family (Neoh et al., 2022). Lemoigne accomplished this by isolating a solid substance extracted from the cells of the gram-positive bacteria *Bacillus megaterium*, under anaerobic conditions, during nutrient starvation (Lenz & Marchessault, 2004). Following that discovery, it was further determined that the synthesis of PHA is not limited to the species *Bacillus megaterium*. For instance, it has been found in microorganisms belonging to the genera *Cupriavidus* (Steinbüchel & Schlegel, 1991), *Micrococus* (Mohanrasu et al., 2021), *Geobacillus* (Giedraitytė & Kalėdienė, 2015), *Alcaligenes* (Wang & Lee, 1997) and many more.

Since the early 1960s, the primary assumption behind the microbiological production of PHA granules has been their capability to convert carbon sources into PHA and subsequently utilize them to produce energy (Samrot et al., 2021). Since then, new studies have been developed to see if there were other functionalities besides the previously studied function that PHA could have in bacteria and archaea (Williams et al., 1999). It was discovered that PHAs were also key metabolites in specific environmental conditions, especially for protecting microorganisms that habit extreme environments (Obruča et al., 2018), such as extremely high/low temperatures (Obruča et al., 2018), high pressure (Obruča et al., 2018), high salinity (Koller, 2017) and other environmental stress-inducing factors.

These PHA granules, also known as "carbosonomes" (Jendrossek et al., 2009; Obruča et al., 2022), formed and retained on the intracellular level by several bacteria and archaea, exhibit a complex structure with a protective coating surface consisting of a phospholipid monolayer comprised with various PHA granule-associated proteins (Vicente et al., 2023). These proteins act as intermediaries between the hydrophobic PHA polymer and the hydrophilic cytoplasm, resulting in structurally simple polyesters with intriguing and advantageous properties for proper performance, development and survivability of the cells (Vicente et al., 2023), such as insolubility in water, relative

resistance to hydrolytic breakdown and strong ultraviolet (UV) resistance (Bugnicourt et al., 2014).

1.3.2. PHA classifications and main characteristics

PHA's classification is often influenced by the composition and structure of the synthesized monomer, determined by the producing microorganism and its growing conditions, as well as the carbon source provided (Kumar & Kim, 2018). PHA polymers consist of monomers known as HAs but can exhibit a variation in the alkyl side chain (R), which can specifically differ in the number of carbon atoms present (Figure 1.3.). The monomer constituents of the PHA are typically chiral 3-hydroxy acids, although the polymer chain can also contain chiral and achiral 2-, 4-, 5- and 6- hydroxy acids (Obruča et al., 2022). It is this variation in the alkyl side chain that accounts for the extensive range of PHA polymers available, which exhibit a wide range of characteristics and functions (Alcântara et al., 2020; Tan et al., 2017). Some studies have found that there are over 150 different types of monomeric building blocks can be incorporated into the polymer chain that can be linked together to form the PHA polymer (Alcântara et al., 2020; Obruča et al., 2020).

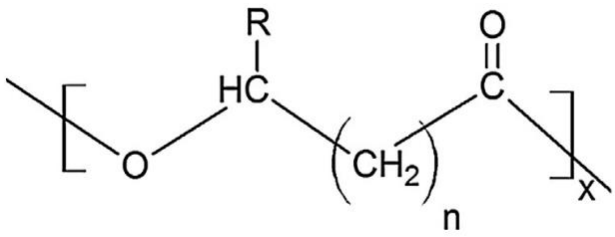

Figure 1.3. - PHA basic structure. R: Type of alkyl side chain. X: Number of methylene groups in the monomer backbone. n: number of polymer chain's repeating units. Adapted from Możejko-Ciesielska and Kiewisz (2016).

PHAs can be divided into groups based on how many carbon atoms make up each monomer unit (Figure 1.4.). The most prevalent PHA among PHA-producing microorganisms is the short-chain length PHAs (scl-PHAs), composed with fewer than five carbons (Wang et al., 2016). The majority of scl-PHAs display thermoplastic capabilities, high crystallinity and high melting points. Medium-chain length PHAs (mcl-PHAs) have five to fourteen carbons. In contrast to scl-PHA, these compounds have significantly lower melting temperatures and poor crystallinity (Alcântara et al., 2020). There can also be over fourteen carbons, namely referred to as the long-chain length

PHAs (lcl-PHAs). But according to Obruča et al. (2022), these lcl-PHAs are almost non-existent in nature.

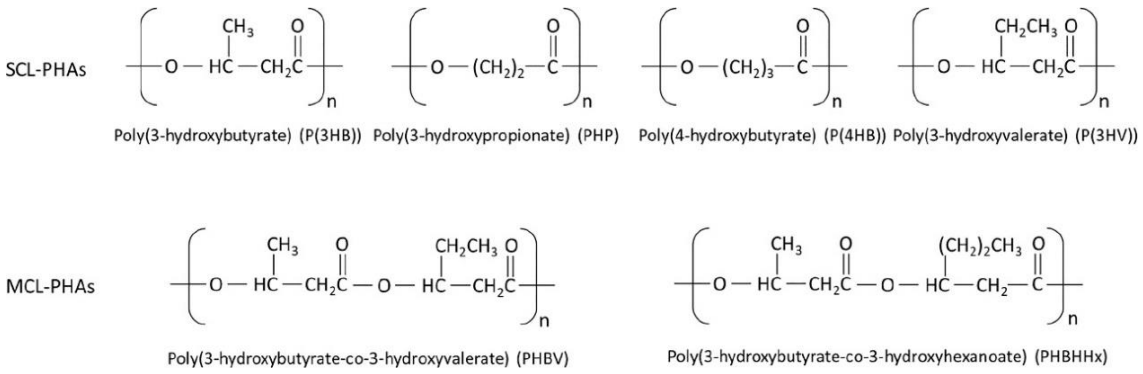

Figure 1.4. - Some selected examples of PHA, according to how many carbon atoms make up each monomer unit. Poly-3-hydroxybutyrate (P(3HB)), poly-3-hydroxypropionate (PHP), poly-4-hydroxybutyrate (P4HB) and poly-3-hydroxyvalerate (P(3HV)) are represented as scl-PHAs. Poly(3-hydroxybutyrate-co-3-hydroxyvalerate) (PHBV) and poly(3-hydroxybutyrate-co-3-hydroxyhexanoate) (PHBHHx) are represented as mcl-PHAs. Adapted from Kaniuk and Stachewicz (2021).

If we are classifying PHA according to the chemical nature of the monomer, they can be divided into 3 parts: PHAs containing aliphatic fatty acids, such as PHB, aromatic fatty acids, such as poly(3-hydroxy-5-phenyl-valerate) (PHPV) and finally, heteropolymers that combine both aliphatic and aromatic fatty acids. Notable examples include poly(3-hydroxybutyrate-co-3-mercaptopropionate) (P(3HB-co-3MP)) and poly(3-hydroxyhexanoate-co-3-hydroxyoctanoate) (P(3HHx-co-3HO)) (Simó-Cabrera et al., 2021).

1.3.3. PHA synthase classification

The term PHA synthase (phaC) is referred to the enzyme that produces PHA. In other words, the synthesis of PHA, inside microorganisms, depends on these enzymes and are in charge of polymerizing the monomers or constituent parts to create the finished PHA polymer chain (Lai et al., 2023). The classification of PHA synthase extends over four distinct categories, determined by the subunit composition (Jia et al., 2016). Enzymes having a molecular weight between 60 and 70 kDa and just one subunit phaC, fall within the category of class I and II. Class III needs two subunits that together make up the phaEC complex, having a molecular weight around 40 kDa: a catalytic phaC class I subunit and a second subunit, phaE class III specific PHA synthase subunit, whose

function is currently unidentified (Neoh et al., 2022). The class IV of PHA synthases comprises two subunits, namely phaC and phaR, the latter being responsible for catalyzing alcohol cleavage of the PHA chain and regulate PHA biosynthesis (Sagong et al., 2018). This class type is found to be present typically in microorganisms belonging to the class *Bacilli* (Obruča et al., 2022). The class IV phaC subunit has a molecular weight of 40 kDa and phaR subunit has 20 kDa (Obruča et al., 2020; Tsuge et al., 2015). Nevertheless, the existing classification of PHA synthases into four distinct classes is currently undergoing adaptation. This is due to the discovery of newly isolated synthases that do not fit within the previously described classes (Tsuge et al., 2015).

1.3.4. PHA biosynthesis and major metabolic pathway

The biosynthetic pathways of PHA are interconnected with the central metabolic pathways of the microorganisms (Alcântara et al., 2020). These include the Krebs Cycle, *de novo* fatty acid synthesis, amino acid catabolism, glycolysis, the Calvin Cycle and the serine pathway (Tan et al., 2014). Acetyl-CoA, being a common intermediate, is shared between PHA pathways and these various metabolic pathways. One prominent example is observed in PHA-producing microorganism *Cupriavidus necator*, where the flow of metabolic flux from acetyl-CoA to PHA is heavily influenced by nutrient availability and environmental conditions (Tan et al., 2014). More specifically, the synthesis of significant quantities of acetyl-CoA from the Krebs cycle blocks PHA synthesis, as it inhibits beta-ketothiolase (phaA), when there is a balance of carbon availability and no other growth-related restriction is present as the Krebs cycle uses acetyl-CoA to provide energy and promote cell development. The acetyl-CoA concentration becomes non-inhibitory, however, if the carbon surplus circumstances are maintained but there is a constraint of some specific nutrients, resulting in the availability of acetyl-CoA to the PHA biosynthesis pathways (Alcântara et al., 2020).

Multiple metabolic pathways can be employed to break down carbon sources used for PHA synthesis. It is known that there are around 14 known metabolic pathways leading to PHA synthesis (Meng et al., 2014). For the sake of simplicity, this work focused on poly-3-hydroxybutyrate P(3HB), the most studied and synthesized PHA globally and its metabolic pathway (Figure 1.5.) (Alcântara et al., 2020). Three distinct enzymes control the stages in the production of this PHA. The first process is based on the condensation of two acetyl-CoA molecules. This condensation is facilitated by phaA and it yields acetoacetyl-CoA. Then, acetoacetyl-CoA is reduced by

NAD(P)H-dependent acetoacetyl-CoA reductases, known as phaB and produces R-3-hydroxybutyryl-CoA, which is then converted by phaC to polymerize P(3HB) (Alcântara et al., 2020). It should be noted that after PHA synthesis, the PHA may be depolymerized after bacteria's nutrients limitations are withdrawn and the normal metabolism conditions for generating energy is reinstated, as PHA depolymerase (phaZ) converts the PHA into energy molecules that are simple to digest (Kessler & Witholt, 2001; Obruča et al., 2020).

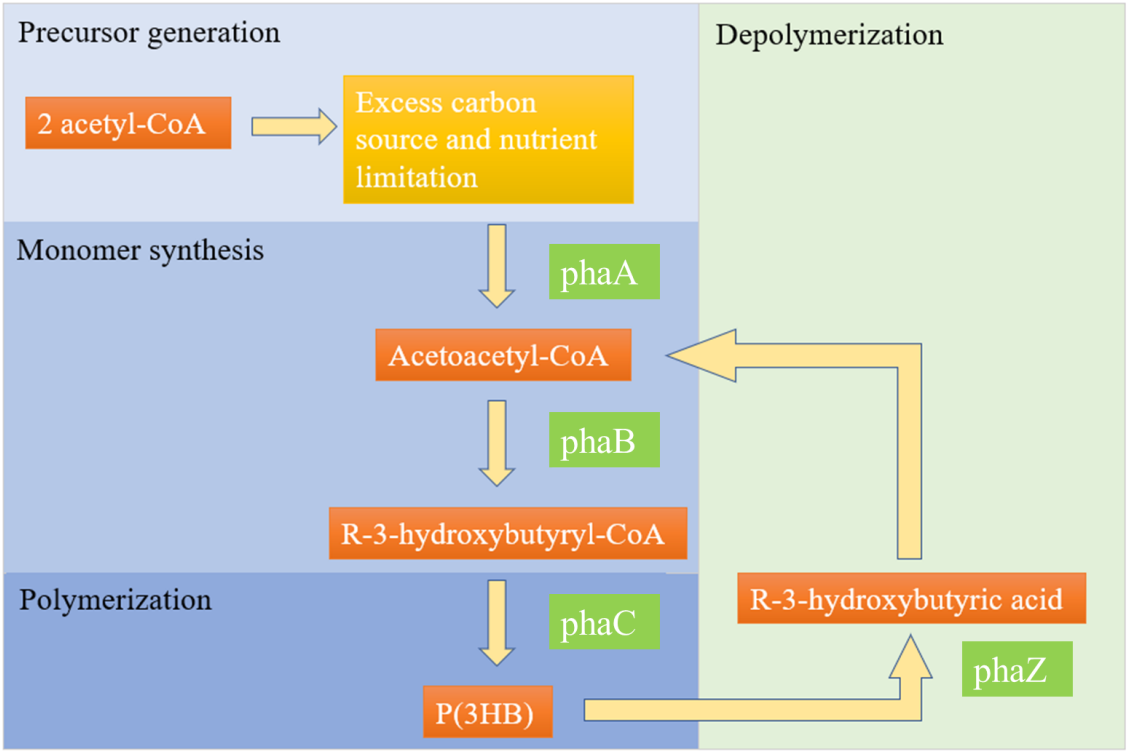

Figure 1.5. -The main metabolic pathway for the P(3HB) synthesis, the most synthesized PHA globally. phaA: beta-ketothiolase. phaB: NAD(P)H-dependent acetoacetyl-CoA reductases. phaC: PHA synthase. phaZ: PHA depolymerase. Adapted from Alcântara et al. (2020).

It is important to emphasize that the processes of production and breakdown of PHA are intimately linked and take place concurrently in the cells. Consequently, even under circumstances that are optimal for PHA production (such as an abundance of carbon substrate, for example), PHA depolymerase can be active to some degree (Obruča et al., 2018; Obruča et al., 2022). Because of this, the metabolism of PHA is sometimes referred to as the "PHA cycle" in a way to highlight the cyclical nature of the process (Prieto et al., 2016). The optimal functioning of the PHA cycle is vital for the survival of bacterial cells. This cycle directly impacts the number of PHA granules within

bacterial cells at any given time, ensuring a controlled supply of carbon for the transient demand of metabolic intermediates (Obruča et al., 2020).

1.3.5. Accumulation of PHA in microorganisms

As already mentioned, the first microorganism to be verified as a PHA producer was *Bacillus megaterium* (Lenz & Marchessault, 2004). Since then, extensive studies have been conducted to comprehend and exploit PHA production in various bacterial and archaeal species, despite it being a relatively unpredictable characteristic among microorganisms. Nonetheless, PHA accumulation has been identified in more than 70 bacterial and archaeal species (Alcântara et al., 2020). Given that many species can accumulate this polymer mainly as an energy reserve in the face of external factors, namely environments where adaptable conditions are difficult to live in and nutrients may be scarce, the aim is usually to discover new species that can live in extreme survival circumstances and have an efficient synthesis of PHA, so that they can then be used in various applications at an industrial and commercial level (Bhola et al., 2021; Obulisamy & Mehariya, 2021).

According to Shahid et al. (2021) and Khanna and Srivastava (2005), PHA-producing species are often divided into two groups depending on the culture conditions adaptability. When there is an additional carbon substrate present and there is a restriction availability to essential nutrients, such as nitrogen, phosphorous, magnesium or sulfur, this first group synthesizes and accumulates PHA. Strains of the genera *Pseudomonas*, *Methylotrophs*, *Protomonas* and *Cupriavidus* are included in this category. For the second group, limitations on nutrition are not necessary to promote PHA accumulation as PHA can be stored by the microbes throughout normal growth. The species *Alcaligenes latus* is one example that fits in this group (Lee et al., 1995; Shahid et al., 2021). It is important to note that although many different bacteria naturally produce PHA, it is also feasible and profitable to create recombinant non-PHA producers such as *Escherichia coli* in order to accumulate PHA (Alcântara et al., 2020; Możejko-Ciesielska & Kiewisz, 2016). Even PHA-producing species can be genetically engineered to grant a higher yield for PHA accumulation. Taking the case of *Cupriavidus necator*, by genetically modifying the species, it was possible to use it effectively as one of the first PHA producers on an industrial scale, being able to accumulate PHA up to 89% of the cellular dry weight (CDW), making PHA production economically viable (Alcântara et al., 2020; Tan et al., 2014). In the case of the genetically modified non-producing species, *Escherichia coli* is

currently one of the most used species in the industry, since in fact, this species has undergone genetic engineering to synthetize PHAs at levels as high as 90% of CDW (Alcântara et al., 2020). In addition to this, this organism has several benefits, including the ability to use a range of affordable carbon sources and the absence of an intracellular PHA depolymerase (Alcântara et al., 2020).

1.3.6. Fermentation methods and strategies for PHA production

Originally, the term "fermentation" was referred solely to an anaerobic biotechnological process like yeast ethanol production and bacteria's lactic acid production. However, today, "fermentation" is also applied to describe aerobic processes, such as the oxygen-dependent production of acetic acid, yeast biomass and PHA, as discussed in this work (Koller, 2018).

For microorganisms to be able to exploit and take advantage of the carbon available in the medium and transform it into intracellular PHA for energy storage and other functions, a fermentation developmental phase must first take place, which is vital to maximize production and save costs (Khanna & Srivastava, 2005). The entire process involves carefully selecting the ideal species for PHA production and evaluating and calculating optimal carbon sources. Initially, ample nutrient sources are provided in the medium, followed by restriction, except for the carbon substrate, to enhance PHA production. It is considered its cost-effectiveness, potential biomass growth, time and performance for PHA synthesis. The development of models for the fermentative production of PHA, in fed-batch, batch and continuous bioreactor units has been the focus of several works published in recent years. These models range in complexity and are adjusted to the type of strain worked on (Karasavvas & Chatzidoukas, 2020).

1.3.6.1. Fed-batch culture

When one or more nutrients are provided to the bioreactor during cultivation and the products are kept in the bioreactor until the conclusion of the run, this operational approach is referred to as fed-batch culture, the most used biotechnological batch procedure for PHA production (Huschner et al., 2015). The process is designed for maximum efficiency in achieving a high yield of PHA and cell concentration. It utilizes an inhibition phase that includes restricting vital nutrients like nitrogen, as well as the presence of an excess substrate, usually a carbon source, which promotes the desired enhanced formation of the intracellular PHA polymer (Yamanè & Shimizu, 1984). In a

fed-batch process, several parameters may also be used to control the growth, such as pH, high glucose concentrations, nitrogen supplies and temperature (Koller, 2018; Shahid et al., 2021).

1.3.6.2. Batch culture

Batch cultivations for PHA production are characterized by simplicity but suffer from low productivity (Koller, 2018). The concentration of nitrogen and carbon sources is limited at the start of fermentation, limiting the possibility of manipulating the process along the fermentation, being at the mercy of the physiological conditions of the microorganisms and the way they consume the substrates initially introduced (Koller, 2018; Stanley et al., 2018). Overall, the conversion yield of carbon sources to PHA is low, making these processes economically unfeasible. Repeated batch approaches have been recently demonstrated to enhance cell biomass productivity, such as the "drain-and-fill" batch culture strategy, which resulted in improved PHA biosynthesis but not as comparable as fed-batch (Koller, 2018).

1.3.6.3. Continuous culture

In continuous processes, a method where microbial cells are continuously cultured and maintained in a steady-state environment and the nutrients and other essential factors are continuously supplied while waste products are continuously removed, is an approach that allows for consistent cell growth and product formation over extended periods, making it suitable for large-scale industrial applications and biotechnological processes. (Koller & Braunegg, 2015). However, because the reaction amount stays steady and usually there is a high amount of nutrients, it might inhibit the growth of the desired PHA or lead to the production of unwanted elements (Koller, 2018).

In such instances, fed-batch operation has been proven to be better compared with both batch cultivation and continuous processes for PHA accumulation and production (Aguirre-Ezkauriatza et al., 2010; Koller, 2018).

1.3.7. Extraction of PHA

The extraction of PHA has already been widely explored over the years as many researchers have looked at various strategies to recover these biopolymers, therefore in this part, some of the frequently used procedures for PHA extraction are covered (Khanna & Srivastava, 2005; Shahid et al., 2021). The choice of approach depends on elements

including the type of strain being employed, the required PHA purity, scalability and costs. To effectively recover biopolymers with the desired characteristics and applications, the extraction method must be assessed and optimized since each extraction process has its own set of benefits and drawbacks (Shahid et al., 2021).

1.3.7.1. Chemical extraction

This method involves the use of solvents or chemical agents to dissolve the PHA biopolymers. Common solvents used include organic ones such as chloroform, an example of a halogenated solvent. This specific solvent is referred to as the standard for PHA extraction since they have been shown to recover a large yield of PHA with a high degree of purity, reaching up to 99% (Koller et al., 2013). This procedure improves cell disruption, solvent permeation and accessibility to PHAs granules while potentially reducing extraction costs. Pre-treating the microbial biomass with sodium hypochlorite (NaClO), commonly known as bleach, significantly enhances PHA recovery, as weakens cell membranes, aiding subsequent PHA extraction with solvents, obtaining the highest extraction yields and purity values. Further enhancement in PHA extraction also can be achieved by combining NaClO pre-treatment with PHA precipitation using alcohols (Koller et al., 2013; López-Abelairas et al., 2015; Ramsay et al., 1990). This approach employs "PHA anti-solvents" pre-treatment like ethanol or methanol to decrease PHA solubility while keeping impurities soluble, making it easier to separate these two components (Koller et al., 2013; Pagliano et al., 2021).

1.3.7.2. Mechanical extraction

Mechanical methods rely on physical forces to separate the biopolymers from the biomass. Techniques such as pressing, grinding or milling are used to break down the biomass and release the biopolymers. Mechanical extraction is relatively simple and cost-effective but may result in lower yields compared to other methods (Shahid et al., 2021).

1.3.7.3. Enzymatic extraction

Enzymes are used to selectively degrade and digest the biomass components and release the biopolymers. Specific enzymes are chosen based on their ability to break down the target biopolymer. Enzymatic extraction offers high selectivity and mild operating

conditions but can be time-consuming and expensive due to the need for specialized enzymes (Shahid et al., 2021).

1.3.7.4. Supercritical fluid extraction

Supercritical fluids, such as supercritical CO_2, are used as solvents to extract PHA biopolymers. These fluids exhibit properties of both liquid and gas and can penetrate the biomass, facilitating the extraction process. Supercritical fluid extraction offers high selectivity, no residue and reduced environmental impact but requires specialized equipment and expertise (Hejazi et al., 2003).

1.3.7.5. Sonication extraction

The sonication method is an advanced technique that combines chemical extraction with the use of ultrasonic waves. It involves mixing cells with hot chloroform and subjecting them to sonication in an ultrasound bath. Subsequently, high-power sonication is applied for several minutes. This method, used together with the chemical extraction method, helps the granules be liquefied using chloroform and the biopolymer is precipitated using ice-cold ethanol. Finally, the precipitated biopolymer is dried in a vacuum oven. While sonication is a useful technique for PHA extraction, it's crucial to remember that it might not be appropriate in every circumstance. Alternative techniques could be required because certain microorganisms have exceptionally strong cell walls that are resistant to sonication (Pradhan et al., 2018).

1.3.8. PHA detection, characterization and quantification methods

The first step for PHA observation involves the screening of PHA-producing microorganisms (Sangkharak & Prasertsan, 2012). One commonly used approach is using a staining method, which allows for the direct visualization of PHA granules within the bacterial cells. By using specific dyes or stains, researchers can identify and differentiate their potential based on their PHA accumulation. These staining methods, such as Sudan Black B and Nile Blue A are the ones employed to visualize intracellular PHA granules (Samrot et al., 2021). Nile Blue A, a hydrophilic oxazine dye, combined with a fluorescence microscope has shown higher precision and better visualization for PHA detection compared to Sudan Black B, as demonstrated by Ostle and Holt (1982). However, Sudan Black B is useful for an economical, fast, first approach to detect these

granules, as they reveal black inclusions of PHA inside the cells, seen through a phase-contrast microscope (Mesquita et al., 2015).

Other microscopy methods, such as scanning electron microscopy (SEM) and transmission electron microscopy (TEM), allow for direct visualization and facilitate the study of the microstructure and morphology of PHA granules (Gupta et al., 2021). Before viewing samples under TEM, they need to be prepared by fixing them in a solution containing glutaraldehyde or paraformaldehyde, followed by osmium tetroxide and uranyl acetate solutions. After dehydration and embedding in resin, the samples are sectioned for TEM imaging. One disadvantage is that TEM can only confirm the presence of granules and not their composition and it requires expensive chemicals and time-consuming sample preparation (Samrot et al., 2021). SEM is another technique that provides high-resolution three-dimensional images of the PHA morphology inside cells without complex sample preparation (Fialová et al., 2017). Researchers have used SEM to investigate the microstructure, surface morphology and chemical composition of PHA produced by several PHA-producing species (Nwinyi & Owolabi, 2019). SEM images of several PHA polymers such as P(3HB) and poly(3-hydroxybutyrate-co-3-hydroxyvalerate) (P(3HB-co-3HV) showed porous materials with regular patterns and microbeads of varying sizes, providing information on the size, shape and distribution of the PHA granules within bacterial cells, aiding in the characterization of PHA-producing microorganisms (Govindasamy et al., 2019). In summary, TEM is useful for studying the internal structure of cells and visualizing PHA granules but has limitations in confirming composition and requires extensive sample preparation. SEM provides detailed 3D images of PHA morphology without the complicated sample preparation.

Spectroscopy methods also play a crucial role in the characterization of PHAs. Such techniques, for example, UV-visible spectroscopy (UV-Vis) and fourier transform-infrared spectroscopy (FT-IR), provide valuable insights into the chemical composition and structure of PHAs (Samrot et al., 2021). Law and Slepecky followed by Williamson and Wilkinson responded by offering a straightforward method UV-Vis methodology (Law & Slepecky, 1961; Williamson & Wilkinson, 1958). Their method involves centrifuging the PHA granules after the PHA-producing cells have been digested in an alkaline sodium hypochlorite solution. Following the use of an adequate solvent to precipitate these granules, sulfuric acid is added to help PHA turn into crotonic acid. In other words, under a temperature of 100ºC, sulfuric acid converts, for example, P(3HB) to 2-butenoic acid (Watanabe et al., 2012). A UV spectrophotometer is then used to find

a peak in the 235 nm wavelength in order to measure the amount of crotonic acid produced as a result of the interaction between PHA and concentrated sulfuric acid.

The other spectroscopy method, FT-IR, has become a useful and quick method for examining microorganisms and their biological components. The chemical structure of PHA and its monomeric components can be better understood using this technique (Novais & Peixe, 2021). The identification of various functional groups inside the PHA molecule by FT-IR involves little sample preparation and makes it easier to distinguish between different PHA kinds based on their distinctive carbonyl absorption properties (Helm et al., 1991). In a study done by Bhuwal et al. (2013), it was discovered that the presence of strong carbonyl marker bands in the 1700 cm^{-1} range may suggest PHA accumulation within cells because hydrogen-bond interactions are caused by the close proximity of the oxygen atoms in the carbonyl group to hydrogen atoms. This method allows researchers to analyze the functional groups present in the polymer and determine its monomer composition (Novais & Peixe, 2021; Samrot et al., 2021).

Chromatography techniques are another important tool for characterizing PHAs. Gas chromatography-mass spectrometry (GC-MS) and high-performance liquid chromatography (HPLC) can be employed to separate and analyze each individual monomer that makes up the PHA polymer. The most popular one for precisely measuring the composition of PHA is GC-MS. Before analysis, the PHA-producing cells must be depolymerized into acids, diols or esters, helping collect the desired high-sensitivity information regarding the monomeric makeup of PHA. Researchers have used GC-MS to detect PHB in cells, by treating them with chloroform, methanol and sulfuric acid to induce methanolysis (Bhuwal et al., 2013). HPLC is an alternative chromatographic method that does not require methanolysis of PHA (Satoh et al., 2016). HPLC, for example, has been used to measure cellular P(3HB) material by treating P(3HB)-accumulated cells with concentrated sulfuric acid, at a temperature of 100°C to convert P(3HB) to crotonic acid (Kichise et al., 2002). Nevertheless, one disadvantage of HPLC is that the polymer must be derivatized (Duvigneau et al., 2021). In summary, GC-MS is commonly used for the exact determination of PHA composition with high sensitivity, while HPLC provides an alternative method that avoids methanolysis but requires the derivatization of the samples. These two techniques enable the determination of the monomer distribution within the polymer chain, which is crucial for understanding the properties and potential applications of the PHA (Samrot et al., 2021).

1.3.9. Biodegradation of PHA

Biodegradation of PHA polymers can occur in both aerobic and anaerobic environments (Jendrossek et al., 1996; Shahid et al., 2021). PHA is degraded aerobically by bacteria that transform organic carbon into CO_2 while exposed to oxygen. In some circumstances, the polymer itself might serve as an alternative supply of oxygen. While aerobic biodegradation has been extensively studied, anaerobic biodegradation (in the absence of oxygen) is less explored due to the complexity of environment control required for research and it does not represent the majority of natural environments where plastic waste could biodegrade (Fernandes et al., 2020; Shahid et al., 2021). However, it is observed that under anaerobic conditions, PHAs experience accelerated degradation under mesophilic circumstances, compared to thermophilic environments, so the mesophilic anaerobic biodegradation for PHAs presents substantial potential as a technique for waste management if plastic finds its way into wastewater treatment systems, leading to methane and CO_2 production, depending on the amount of oxygen present in the environment or the type of material being decomposed, which is a potent greenhouse gas leading for commercial use (Fernandes et al., 2020).

Microorganisms play a crucial role in the biodegradation of PHA-based plastics across various environments. There are two different kinds of microorganisms involved in biodegradation: those that physically break down PHAs and those that digest the residues of that breakdown such as butyric acid and valeric acid. This process relies on microorganisms producing PHA depolymerases, which break down water-insoluble PHA into soluble forms that can be utilized. Soil-based PHA biodegradation rates are influenced by factors like microbial community composition and the specificity of the produced depolymerases. Rough surfaces facilitate microbial adhesion and water interaction, enhancing polymer biodegradation (Fernandes et al., 2020; Purushothaman et al., 2001). Numerous microorganisms have been identified for PHA degradation, with almost 600 depolymerases classified into distinct superfamilies and families. Species of bacteria from the genera *Stenotrophomonas*, *Alcaligenes*, *Comamonas* and *Rhodococcus* as well as fungi including genera *Ascomycetes* and *Aasidiomycetes* demonstrate PHA-degrading potential as certain microorganisms specialize in degrading specific PHA types, while others can target multiple PHAs due to their versatile depolymerase production (Emadian et al., 2017; Fernandes et al., 2020).

1.3.10. PHA biotechnological applications and current trends

Due to the vast spectrum of types of monomers, different species of microorganisms produce different types of PHA, namely different types of scl-PHA and mcl-PHA, these two groups have also different purposes for different industrial applications, each one having their unique advantages and disadvantages (Możejko-Ciesielska & Kiewisz, 2016), making them useful for a number of products such as in the field of packaging, agriculture, molding products, coatings agent, medical devices and in nanotechnology (Bedade et al., 2021; Samrot et al., 2021; Shahid et al., 2021).

As said earlier, scl-PHAs are highly crystalline, with a typical crystallinity range of 55-80% (Możejko-Ciesielska & Kiewisz, 2016). They are completely stereoregular polyesters with high melting temperatures (173-180°C) and low glass transition temperatures (5-9°C), resulting in a relatively stiff but easily breakable material. These temperature parameters are important for determining the suitability of scl-PHAs in various applications, as they define the temperature limits for potential commercial use (Możejko-Ciesielska & Kiewisz, 2016; Obruča et al., 2018). Scl-copolymers, such as P(3HB-co-3HV), exhibit better properties compared to scl-homopolymers. The qualities of the material may be changed by adding different monomers to the copolymer chain. Researchers may modify the PHA copolymer to have particular properties, including increased flexibility, thermal stability or biodegradability. The copolymers have lower melting points, reduced crystallinity and are easier to mold, making them more desirable, as scl-PHAs by themselves are not very useful on a commercial level (Możejko-Ciesielska & Kiewisz, 2016; Obruča et al., 2018). Scl-copolymers are promising as a packaging material, as they can be processed into bottles and bags, replacing the petroleum-based plastics currently used (Możejko-Ciesielska & Kiewisz, 2016; Obruča et al., 2020).

On the other hand, mcl-PHAs exhibits "elastic" properties, within a narrow temperature range as they have a lower melting temperature range of 39-61°C, have a glass transition temperature below room temperature and are about 25% crystalline. These combined attributes give greater malleability of mcl-PHAs when compared to scl-PHAs. This greater malleability allows mcl-PHAs to adapt and flex more quickly in response to mechanical forces and environmental conditions (Możejko-Ciesielska & Kiewisz, 2016). The properties of mcl-PHA are suitable for a variety of applications, such as coating, agriculture, pharmacy, chemistry, medical usage and agriculture (Shahid et al., 2021). More specifically, in the medical field, mcl-PHAs are used in surgical mesh,

sutures, stents and drug delivery systems (Oryan et al., 2014). In agriculture, mcl-PHAs are also employed in biodegradable mulch, greenhouse films, nets for crop protection and grow bags (Shamsuddin et al., 2017). mcl-PHAs also exhibit antimicrobial properties, an additional property useful for implant coatings and food packaging (Rodríguez-Contreras et al., 2019). In terms of coating, they can be used as biodegradable packaging materials, providing moisture and oxygen barriers for food items. They are water-resistant, making them suitable for products like diapers, milk cartons and feminine hygiene products (Basumatary et al., 2020). Nowadays, more innovative ways to apply PHA are emerging as a result of considerable efforts in the development of new technologies in the area of biotechnology, namely, in regenerative or self-healing PHA biopolymers and nanoparticles (Samrot et al., 2021).

1.3.11. PHA role in extremophile species

A wide variety of bacteria and archaea, distinguished by their capacity to accumulate PHA, exhibit remarkable abilities in environments that pose challenges to normal survival, demonstrating the fundamental importance of PHA in ensuring the survivability of extremophile microorganisms under adverse conditions (Obruča et al., 2018). These challenges may arise from extreme temperature fluctuations, high levels of radiation, elevated salinity or extreme pH levels, as already mentioned. Despite such inhospitable conditions, the presence and accumulation of PHA within these microorganisms enable them to not only endure but also flourish (Obruča et al., 2022).

Halophile microorganisms are one of the most investigated PHA producers among extremophiles. The PHA accumulation appears to be a characteristic shared by a variety of strains that thrive in excessively salty conditions, including both haloarchaea and halophilic bacteria (Obruča et al., 2020; Sedlacek et al., 2019). It was hypothesized that the main purpose of these PHA granules on halophiles was to decrease the cytosol volume to lower the energy need of cells for osmotic homeostasis and as a result, the PHA demonstrates a crucial role for the cells to handle the environments where only halophiles can survive (Saponetti et al., 2011).

Other extremophile microorganisms that take advantage of the accumulation of PHA for survivability are thermophilic microorganisms (Kouřilová et al., 2021; Obruča et al., 2020). No hypothesis has been debated regarding the direct link between the accumulation of PHA in thermophilic species and the extreme temperatures, as these are still poorly studied (Obruča et al., 2020). Nonetheless, various hypotheses have been put

forth to elucidate how microorganisms adapt to high-temperature environments. These hypotheses often involve mechanisms like the accumulation of molecular chaperones to shield biomolecules from thermal denaturation and the preservation of membrane integrity under extreme heat conditions (Urbieta et al., 2015).

Due to the challenges linked to high-temperature cultivation practices, such as decreased oxygen solubility at higher temperatures and the high amount of energy required to keep high cultivation temperatures, industrial and biotechnological execution of thermophilic bacteria strains may appear to be unrealistic at first glance (Koller, 2017; Obruča et al., 2022). This is due to the fact that high-temperature cultivations require a lot of energy to maintain (Obruča et al., 2020; Sedlacek et al., 2019). However, the growth of thermophilic species in bioreactors can greatly improve energy efficiency by reducing the need for cooling, which is typically energy intensive (Obruča et al., 2020). Additionally, working with thermophilic organisms allows for minimizing energy-intensive sterility procedures (Sedlacek et al., 2019). It was thought that only some specific thermophilic species could synthesize PHA, as many other that were studied, was not recorded at all, in contrast to halophiles, suggesting either that thermophilic PHA biosynthesis is still not well understudied or that thermophilic PHA biosynthesis is not as prevalent as it is in halophiles (Sedlacek et al., 2019). However, the species of the genus *Rubrobacter*, are promising contenders for PHA synthesis on an industrial scale among prospective thermophilic candidates for biotechnological application (Kouřilová et al., 2021).

1.4. The genus *Rubrobacter*

The genus *Rubrobacter*, one of the descendant lines of the phylum *Actinomycetota* (Oren & Garrity, 2021), was first described by Suzuki et al. (1988), with its first species being *Rubrobacter radiotolerans*, in which enormous resistance to radiation induction was observed in the microorganism, the reason why this species has this peculiar name (Suzuki et al., 1988; Yoshinaka et al., 1973). Later on, more species from this genus were described. In general, these species typically thrive in aerobic conditions, are gram-positive, are nonmotile and do not form endospores as part of their life cycle (Castro et al., 2019; Suzuki et al., 1988).

To date, there are eleven type species with validly published names under the International Code of Nomenclature of Prokaryotes (ICNP), these being *Rubrobacter aplysinae* (Kämpfer et al., 2014), *Rubrobacter bracarensis* (Jurado et al., 2012),

Rubrobacter calidifluminis (Albuquerque et al., 2014), *Rubrobacter indicoceani* (Chen et al., 2018), *Rubrobacter marinus* (Chen et al., 2020), *Rubrobacter naiadicus* (Albuquerque et al., 2014), *Rubrobacter radiotolerans* (Suzuki et al., 1988), *Rubrobacter spartanus* (Norman et al., 2017), *Rubrobacter taiwanensis* (Chen et al., 2004), *Rubrobacter tropicus* (Chen et al., 2020) and *Rubrobacter xylanophilus* (Carreto et al., 1996).

It is known that some of these species can survive in various extreme environments. One example is the species *R. bracarensis*, a halophile that is capable of growth in large ranges of NaCl concentration, with up to 30% NaCl (Albuquerque et al., 2014; Jurado et al., 2012). This organism was isolated from a green biofilm coating the biodegraded wall, inside of a monument (Jurado et al., 2012). Several species of the genus can be classified as thermophilic on which their optimal growth temperature is around 60ºC, including *R. xylanophilus*, *R. calidifluminis*, *R. naiadicus* and *R. taiwanensis* (Albuquerque et al., 2014; Carreto et al., 2016; Chen et al., 2004). In the case of the *R. radiotolerans* and *R. spartanus*, they can be classified as moderate thermophilic, due to their optimal growth temperatures being between 45-50ºC (Norman et al., 2017; Suzuki et al., 1988). These organisms possess biochemical features that allow them to thrive in environments characterized by high temperatures.

1.4.1. Relationship between *Rubrobacter* species and PHA accumulation

The first insight into PHAs accumulation in genus *Rubrobacter* was presented by Kouřilová et al. (2021). Based on information acquired from genomes available in public databases, these authors searched and found various genes involved in PHA synthesis (*phaC*, *phaE)* and in PHA depolymerization (*phaZ)*. The first link between PHA biosynthesis identified at the genotype and phenotype levels was created, as there was indeed PHA accumulation in their experiments. It was determined that the P(3HB) monomer was synthetized in two species of the genus *Rubrobacter*, namely *R. xylanophilus* DSM 9941^{T} and *R. spartanus* DSM 102139^{T}. In the same work, some parameters were discussed in relation to the results obtained. The ability to accumulate P(3HB) with various inexpensive carbon sources, such as glucose and glycerol, was not related to biomass concentration, since, for example, in *R. spartanus* there was a higher biomass accumulation with glucose as a carbon source but in turn, a higher P(3HB) accumulation was detected with glycerol. Regarding PHA accumulation and temperature, there is indeed a correlation between the optimal growth temperature and the

accumulation of the biopolymer. The two species studied showed a better accumulation of PHA at the optimum growth temperature. The PHA accumulation by *R. xylanophilus* didn't get affected by small changes in the temperature of growth, standing as a greater candidate for commercial applications and a standard for further comparisons within the *Rubrobacter* genus (Kouřilová et al., 2021). In accordance with their work, other species of the genus *Rubrobacter* also possess a high level of PHA production potential. Even though not every member has their whole genome sequenced, based on those that are and given that these genes are present, it is expected that all can accumulate PHA at the intracellular level (Kouřilová et al., 2021).

1.5. Objectives

The main objective of this work is to explore PHA synthesis potential in unexamined *Rubrobacter* species. This objective encompasses several key steps. Firstly, the investigation involves a comprehensive analysis of the genomes of *Rubrobacter* species in order to identify and compare the genes involved in PHA production. Subsequently, it involves the experimental validation of PHA production through the selection of optimal growth media to promote biomass growth and consequently the use of a medium for improved PHA accumulation. Lastly, the research aims to visualize and detect the presence of PHA in the selected species through staining, microscopic and indirect PHA detection methods. By establishing a link between the observed phenotypic traits and the corresponding genotypic characteristics, this work seeks to provide an understanding of the potential for PHA accumulation in a wider range of *Rubrobacter* species by searching the presence of specific genes in the genome sequences. The results of this study could pave the way for innovative uses of PHA synthesized by this genus in various industries, contributing to a more environmentally friendly future.

2. Materials and methods

2.1. Microorganism selection

Rubrobacter aplysinae CECT 8425^T, *Rubrobacter bracarensis* CECT 7924^T, *Rubrobacter calidifluminis* RG-1^T, *Rubrobacter naiadicus* RG-3^T, *Rubrobacter radiotolerans* DSM 5868^T, *Rubrobacter radiotolerans* RSPS-4, *Rubrobacter taiwanensis* LS-293^T and *Rubrobacter xylanophilus* DSM 9941^T were the selected species for phenotypic analysis. *Escherichia coli* ATCC 25922 species was used for phenotypic comparative purposes. These organisms were provided by the Private Culture Collection of the Center for Neuroscience and Cell Biology (CNC), in UC-Biotech. In addition to the species mentioned, the genome of the species *Rubrobacter tropicus* SCSIO 52909^T, *Rubrobacter marinus* SCSIO 52915^T and *Rubrobacter indicoceani* SCSIO 08198^T were analyzed for the bioinformatic approach. The genetic information for all the species was retrieved from the GenBank (Sayers et al., 2020) public database.

2.2. *In silico* analysis of genes involved in PHA synthesis

A manual investigation using the Basic Local Alignment Search Tool (BLAST) (Benson et al., 2012) was undertaken to search genes and putative genes (*phaA, phaB* and *phaC*) and thereby identify the corresponding enzymes they encode (phaA, phaB and phaC) in selected *Rubrobacter* species with the whole genome sequenced: *Rubrobacter aplysinae* CECT 8425^T (accession Nº: NZ_LEKH01000011.1), *Rubrobacter calidifluminis* RG-1^T (accession Nº: NZ_JAQKGV010000001.1), *Rubrobacter indicoceani* SCSIO 08198^T (accession Nº: NZ_CP031115.1), *Rubrobacter marinus* SCSIO 52915^T (accession Nº: NZ_CP045121.1), *Rubrobacter naiadicus* RG-3^T (accession Nº: NZ_JAQKGW010000006.1), *Rubrobacter radiotolerans* DSM 5868^T (accession Nº: NZ_FWWX01000004.1), *Rubrobacter radiotolerans* RSPS-4 (accession Nº: NZ_CP007514.1), *Rubrobacter taiwanensis* LS-293^T (accession Nº: NZ_SKBU01000004.1), *Rubrobacter tropicus* SCSIO 52909^T (accession Nº: NZ_CP045119.1) and *Rubrobacter xylanophilus* DSM 9941^T (accession Nº: NC_008148.1). Also, with the tool BLAST, the percentage of identity between *R. xylanophilus* DSM 9941^T phaA and phaB aminoacids sequences with the other *Rubrobacter* species was determined to gain insights into their level of identity. To examine the sequence similarities of PHA synthase subunits (phaC subunit class I and class III), multiple sequence alignments of the amino acid sequences were performed using Clustal Omega tool within the MEGA11 software (Tamura et al., 2021).

Furthermore, an in-depth analysis of the protein-conserved regions was carried out and presented using the online tool ESPript 3.0 (Robert & Gouet, 2014).

2.3. Growth media

2.3.1. Culture conditions optimization

For bacterial cultivation, an optimization procedure was conducted with both *Thermus* medium (Carreto et al., 1996) (Table 2.1. A and B) and Tryptic soy broth (DIFCO) (Table 2.2.), where *R. xylanophilus* DSM 9941^T and *R. radiotolerans* DSM 5868^T were the selected species for this experiment. The media were sterilized in an autoclave at 120ºC, for 15 min. The *Thermus* solid medium (with agar) was evenly distributed onto plastic Petri plates and left to cool down, making them ready for use. The isolates, stored at -80ºC, were unfrozen and streaked on the previously prepared agar plates with *Thermus* medium and incubated in a laboratory oven (EHRET), at their respective described optimal growth temperature: *R. xylanophilus* DSM 9941^T at 60ºC (Carreto et al., 1996) and *R. radiotolerans* DSM 5868^T at 45ºC (Suzuki et al., 1988), until the formation of isolated colonies was visible. Each species colonies were used as inoculum and transferred to three different 250 mL Erlenmeyer flasks containing 100 mL of *Thermus* liquid medium (without agar) supplemented by the respective tryptone and yeast extract concentrations (1 g/L, 2.5 g/L and 5 g/L) and to a 250 mL Erlenmeyer flask containing 100 mL of Tryptic soy broth medium and were left to grow under constant 140 RPM, in a rotary shaker bath (Innova 3100 Digital Water Bath Shaker), at their optimal growth temperature, as mentioned above. In the same conditions, each species was also left to grow at a temperature of 50ºC, for comparative purposes. The growth was then monitored by measuring the turbidity of the culture, at 610 nm, with a UV/Vis spectrophotometer (JENWAY 6405 UV/Vis. spectrophotometer). Then, the growth curve was plotted and the specific growth rate was determined, for each condition.

2.3.2. Growth media for biomass production

Following optimization, *Thermus* medium supplemented by 1 g/L of tryptone and yeast extract concentrations emerged as the preferred choice for biomass production (Table 2.1. A and B**)**. In addition to the isolates used above, the remaining isolates were streaked and incubated in the same way as mentioned above in point 2.3.1., at their optimum growth temperature (*R. aplysinae* CECT 8425^T and *R. bracarensis* CECT 7924^T at 30ºC (Jurado et al., 2012; Kämpfer et al., 2014); *R. radiotolerans* RSPS-4 at 45ºC

(Suzuki et al., 1988); *R. calidifluminis* RG-1^T, *R. naiadicus* RG-3^T, *R. taiwanensis* LS-293^T at 60ºC (Albuquerque et al., 2014; Carreto et al., 1996; Chen et al., 2004), until the formation of isolated colonies was visible. Each species colonies were used as inoculum and transferred to a 250 mL Erlenmeyer flask containing 100 mL of *Thermus* liquid medium. For *R. bracarensis* CECT 7924^T, the medium was supplemented with 3% NaCl. Growth was done under the same constant conditions as 2.3.1., for 24 hours, for the *R. radiotolerans* DSM 5868^T, *R. radiotolerans* RSPS-4, *R. calidifluminis* RG-1^T, *R. naiadicus* RG-3^T, *R. taiwanensis* LS-293^T and *R. xylanophilus* DSM 9941^T species and for 120 hours, for *R. aplysinae* CECT 8425^T and *R. bracarensis* CECT 7924^T species, at their optimal growth temperatures. The growth was monitored under the same conditions as 2.3.1. The growth curve was plotted and the specific growth rate was determined for each condition.

Table 2.1. A - *Thermus* medium, pH 7.0 (Carreto et al., 1996).

Composition
100 mL macronutrients solution 10x
10 mL micronutrients solution 100x
10 mL $FeCl_3.6H_2O$ solution 100x
1 g tryptone
1 g yeast extract
20 g agar

Table 2.1. B - *Thermus* medium concentrated solutions.

Composition of the concentrate solution	g/L
Macronutrients solution 10x:	
Nitrilotriacetic acid (NTA)	1.0
$CaSO_4.2H_2O$	0.6
$MgSO_4.7H_2O$	1.0
NaCl	0.08
KNO_3	1.03
$NaNO_3$	6.89
Na_2HPO_4	1.11
Micronutrients solution 100x:	
$MnSO_4.H_2O$	0.220
ZnSO4.7H2O	0.05
H_3BO_3	0.05
$CuSO_4.5H_2O$	0.0025
$Na_2MoO_4.2H_2O$	0.0025
$CoCl_2.6H_2O$	0.0046
$FeCl_3.6H_2O$ solution 100x	0.0046

Table 2.2. - Tryptic soy broth medium (DIFCO), pH 7.0.

Composition	g/L
Glucose	2.5
NaCl	5
K_2HPO_4	2.5
Soytone	3
Tryptone	17

2.3.3. Growth media for enhanced PHA accumulation

The cultures previously used for biomass growth were transferred and used as inoculum for enhanced PHA accumulation experiments in a mineral salt medium (MSM) (Kouřilová et al., 2021). The composition of this medium is described in Table 2.3. Glucose was selected as the carbon source to supplement the MSM. The culture growth was performed in 250 mL Erlenmeyer's flasks containing 100 mL liquid MSM and were left to grow in the same constant conditions as 2.3.1., for 48 hours, for the *R. radiotolerans* DSM 5868^T, *R. radiotolerans* RSPS-4, *R. calidifluminis* RG-1^T, *R. naiadicus* RG-3^T, *R. taiwanensis* LS-293^T and *R. xylanophilus* DSM 9941^T species, at their optimal growth temperatures. The growth of each species was monitored in the same way as 2.3.1. The growth curve was plotted and the specific growth rate was determined for each condition.

Table 2.3. - MSM, pH 7.0 (Kouřilová et al., 2021).

Composition	g/L
$Na_2HPO_4.12\ H_2O$	9.0
KH_2PO_4	1.5
NH_4Cl	1.0
$MgSO_4.7\ H_2O$	0.2
$CaCl_2.2\ H_2O$	0.02
$Fe(III)NH_4$citrate	0.0012
Yeast extract	0.5
Trace element solution: (EDTA (50.0 g/L), $FeCl_3.6\ H_2O$ (13.8 g/L), $ZnCl_2$ (0.84 g/L), $CuCl_2.2\ H_2O$ (0.13 g/L), $CoCl_2.6\ H_2O$ (0.1 g/L), $MnCl_2.6\ H_2O$ (0.016 g/L), H_3BO_3 (0.1 g/L)	(1 mL/L)
Glucose	20

2.4. Staining techniques

2.4.1. Plate assay

PHA granules were initially identified by examining, with the naked eye, stained bacterial colonies utilizing a modified Sudan Black B staining technique. This technique serves as a rapid screening method for the detection of PHA granules (Liu et al., 1998). *R. radiotolerans* RSPS-4, *R. calidifluminis* RG-1^T, *R. naiadicus* RG-3^T and *R. xylanophilus* DSM 9941^T were the selected species for this experiment. All of them were cultivated in *Thermus* solid medium supplemented with 2% glucose. The bacteria were distributed in three equal portions, on two agar plates. In one plate, two of the three equal parts were inoculated with *R. radiotolerans* RSPS-4 and were then incubated for 72 hours, at 37°C. In the same plate, *E. coli* ATCC 25922 was also introduced, as a negative control, for comparative purposes. In another plate, *R. calidifluminis* RG-1^T, *R. naiadicus* RG-3^T and *R. xylanophilus* DSM 9941^T were equally distributed and incubated for 72 hours, at 60°C. After growth, the colonies were covered with filtrated 0.3% Sudan black B stain in ethylene glycol and were left untouched, on the plates, for 30 min. Then, in order to get rid of the extra tint from the colonies, the plates were lastly cleaned with water and ethanol 96%. Bacterial colonies retaining a dark tint after staining were identified as bacteria capable of accumulating PHA. On the other hand, colonies that did not retain the stain were categorized as negative for PHA accumulation (Mascarenhas & Aruna, 2017).

2.4.2. Sudan black staining

For a better visualization of the PHA granules within the cells, the main Sudan black B staining technique was performed (Wei et al., 2011). *R. radiotolerans* DSM 5868^T, *R. radiotolerans* RSPS-4, *R. xylanophilus* DSM 9941^T, *R. taiwanensis* LS-293^T, *R. calidifluminis* RG-1^{T,} *R. naiadicus* RG-3^T, *R. bracarensis* CECT 7924^T and *R. aplysinae* CECT 8425^T were the selected species for this experiment. For each *Rubrobacter* species, a sample was extracted after 48 hours, in MSM and after 120 hours, in *Thermus* medium, in the case of *R. aplysinae* CECT 8425^T and *R. bracarensis* CECT 7924^T. Smears were prepared on a glass slide, heated and fixed with a Bunsen burner flame and dyed for 10 min. with filtrated 0.3% Sudan Black B stain in ethylene glycol. The slide was then submerged in xylol until it was fully decolorized. A safranin solution (2.5% (p/v) in ethanol 96%) was used as a counterstain, for 5 min., before being rinsed with water. After drying the slides, the samples were ready to be analyzed by optical microscopy.

2.5. Microscope analysis

2.5.1. Optical microscopy visualization of the PHA granules

First, the visualization of the granules of PHA was done by optical microscopy. After the sample preparation with the Sudan black B staining technique, it was added a few drops of immersion oil, on top of the glass slide. After, the samples were observed under an optical microscope (Carl Zeiss Axio Imager A2 and LEITZ), with a magnification of 1000x (Legat et al., 2010). To prevent pigment residues on the smear from compromising with the detection of the cells and the visualization of the PHA granules, a photomicrograph is taken, for each sample, for qualitative analysis, to understand the presence of the PHA granules within the cells. The observation of the photomicrograph was made under a computer and with the help of the ZEISS ZEN Microscopy Software (ZEISS, 2023), it was possible to adjust the contrast, colors and exposure of the image for better visualization of the images.

2.5.2. Transmission electron microscopy

To gain a better image of the PHA granules, a TEM was used for a more detailed observation of the cells, enabling a more definitive conclusion about PHA accumulation. For each sample, 1mL of suspension was extracted directly from each corresponding growing phase (24h and 48h) and was centrifuged at 3000 RPM, for 3 min., for *pellet* formation. The supernatant was discarded and then, a TEM fixation protocol was initiated

to fix the samples (Obruča et al., 2017). A cacodylate buffer solution (0.1 M, pH 7.2) was initially prepared and it was used to dilute the 25% glutaraldehyde to get a final fixative solution, with a glutaraldehyde concentration of 2.5%. The fixation lasted around 3 hours, at 4ºC. In the end, the supernatant was discarded and then only cacodylate buffer solution was added, at 4°C, keeping the samples stable for shipment to the microscopy core facility, in the Instituto de Ciências Biomédicas Abel Salazar (ICBAS), Universidade do Porto, where the samples were prepared and images were taken.

2.6. PHA extraction and detection technique

2.6.1. Halogenated solvent PHA extraction

To extract and detect PHA accumulation in species of the genus *Rubrobacter*, a modified halogenated solvent extraction method was selected, based on the assay developed by Law and Slepecky (1961). This method is well-established and widely employed for PHA detection, ensuring robust and reliable results (Pagliano et al., 2021).

Each species was subjected to sample extraction during their respective growing phases. After 48 hours of growth in MSM for all species except in the case of *R. aplysinae* CECT 8425^{T} and *R. bracarensis* CECT 7924^{T}, which were extracted after 120 hours in *Thermus* medium growth and *E. coli* ATCC 29922 cells were analyzed after 24 hours, cultivated in LB medium (Cultimed), at 37ºC. After growth, 45 mL suspension sample was transferred to a 50 mL Falcon tube, followed by centrifugation at 4000 RPM, for 45 min., at 4ºC. Then, the supernatant was discarded and the pellet was washed with 45 mL of 10 mM Tris-HCL pH 8.0. It was then centrifuged at 4000 RPM, at 4ºC, for 45 min. Then, most of the supernatant was discarded and the pellet was placed in a pre-weighed Petri dish and was dried, in a laboratory hoven (EHRET), overnight, at 100ºC. 50 mL of commercial bleach (13% chlorine) was added to the Petri dish to resuspend the dry pellet. The resuspended pellet was added into a new 50 mL falcon tube and left, in a laboratory oven, overnight, at 37ºC. The falcon tube was then centrifuged at 4,000 RPM, at 4ºC, for 45 min. The supernatant was discarded and the pellet was washed with sterilized distilled water. The pellet was recovered by centrifugation at 4000 RPM, 4ºC, for 45 min. Then, the supernatant was discarded and 10 mL of pure ethanol and 10 mL of pure acetone were added into the falcon tube with the pellet and again centrifuged at 4000 RPM, 4ºC, for 45 min. The supernatant was then discarded and the pellet was resuspended with 10 mL of chloroform and the mixture was introduced to a 250 mL glass flask. This glass flask, with

the solution, was submerged in a water bath at 60ºC until the chloroform was completely evaporated, leaving a white precipitate.

2.6.2. PHA detection

For PHA detection, the previous precipitate was treated with 10 mL of sulfuric acid 99% (H_2SO_4), by heating at 100°C, in a water bath, for 10 min, to obtain crotonic acid. About 2 mL from each sample were transferred to a quartz cuvette and PHA was detected within the expected peak, at 235 nm. Absorbance measurements at 200 nm, 220 nm and 260 nm were also registered against sulfuric acid as a blank (Law & Slepecky, 1961). The Jenway 6405 UV/Vis. spectrophotometer (Jenway) was used for the absorbance measurements.

3. Results

3.1. Identification of PHA-related genes in the *Rubrobacter* genus

In a previous work, the entire genome sequence of several *Rubrobacter* species were examined, leading to the identification of multiple hits regarding enzymes responsible for PHA synthesis (Kouřilová et al., 2021). Since then, in this genus, more species were completely sequenced, leading to an opportunity to expand the knowledge of the mechanisms behind it.

In this section, the research initially began with the identification of the *phaA*, *phaB* and *phaC* genes involved in the PHA biosynthetic pathway (Alcântara et al., 2020).

3.1.1. PhaA

The analysis started with the phaA enzyme, coded by the *phaA* gene, as it holds a central role as the starting point for the main metabolic pathway for PHA synthesis (Alcântara et al., 2020). The phaA can be referred to by various names, including beta-ketothiolase, acetyl-CoA C-acetyltransferase, acetoacetyl-CoA thiolase or even as thiolase family protein (EC 2.3.1.9). *R. xylanophilus* DSM 9941^T *phaA* encoded protein was chosen for comparison with other *phaA* encoded protein *Rubrobacter* species to determine the percentage of identity.

At the amino acid level, a significant similarity was noticed within the *Rubrobacter* genus (Table 3.1.). *R. calidifluminis* RG-1^T and *R. naiadicus* RG-3^T exhibited a percentage of identity of 86.32% and 86.07%, respectively, when compared to the phaA amino acid sequence of *R. xylanophilus* DSM 9941^T. *R. marinus* SCSIO 52915^T and *R. aplysinae* CECT 8425^T species had the lowest percentage of identity, with values reaching 79.85% and 78.61%, respectively.

Table 3.1. - Similarity and comparison between the phaA amino acid sequence of *R. xylanophilus* DSM 9941^T and the phaA amino acid sequences found in other selected *Rubrobacter* species. The information was retrieved from the GenBank public database.

***Rubrobacter* species**	**Protein Accession Nº**	**Nº of amino acids**	**Percent identity**
***R. xylanophilus* DSM 9941^T**	**WP_011565330.1**	**402**	**100.00%**
R. aplysinae CECT 8425^T	WP_047865911.1	400	78.61%
R. calidifluminis RG-1^T	WP_273841767.1	402	86.32%
R. indicoceani SCSIO 08198^T	WP_119069253.1	402	82.09%
R. marinus SCSIO 52915^T	WP_228281425.1	402	79.85%
R. naiadicus RG-3^T	WP_273887804.1	402	86.07%
R. radiotolerans DSM 5868^T	WP_038680622.1	402	83.83%
R. radiotolerans RSPS-4	WP_038680369.1	391	80.05%
R. taiwanensis LS-293^T	WP_207890270.1	400	83.80%
R. tropicus SCSIO 52909^T	WP_166173877.1	402	80.85%

3.1.2. PhaB

The phaB enzyme, coded by the *phaB* gene, which is responsible for the second step for PHA synthesis in the main metabolic pathway, was also analyzed to understand if it is present in the various selected species of the genus *Rubrobacter* and elucidate its existence in the metabolic machinery. The phaB enzyme is also known by the name 3-oxoacyl-[acyl-carrier-protein] reductase or NADPH-dependent acetoacetyl-CoA reductase (EC 1.1.1.36). Here as well, *R. xylanophilus* DSM 9941^T was chosen for comparison with other *Rubrobacter* species to determine the percentage of identity between them (Table 3.2.).

The *R. tropicus* SCSIO 52909^T and *R. marinus* SCSIO 52915^T were identified as the species with a higher percentage of identity compared with the *R. xylanophilus* DSM 9941^T phaB amino acid sequence, reaching values of 81.05% and 79.59%, respectively. On the other hand, both *R. radiotolerans* strains and *R. indicoceani* SCSIO 08198^T got the lowest percentage of identity, with both of the *R. radiotolerans* species showing a value of 73.39% and *R. indicoceani* SCSIO 08198^T, an identity of 70.16%.

Table 3.2. - Similarity and comparison between the phaB amino acid sequence of *R. xylanophilus* DSM 9941^T and the phaB amino acid sequences found in other selected *Rubrobacter* species. The information was retrieved from the GenBank public database.

***Rubrobacter* species**	**Protein accession Nº**	**Nº of amino acids**	**Percent identity**
***R. xylanophilus* DSM 9941^T**	**WP_011564361.1**	**248**	**100.00%**
R. aplysinae CECT 8425^T	WP_047865838.1	248	77.42%
R. calidifluminis RG-1^T	WP_273846703.1	248	79.03%
R. indicoceani SCSIO 08198^T	WP_205544225.1	248	70.16%
R. marinus SCSIO 52915^T	WP_166396613.1	246	79.59%
R. naiadicus RG-3^T	WP_273889147.1	248	77.42%
R. radiotolerans DSM 5868^T	WP_198024445.1	248	73.39%
R. radiotolerans RSPS-4	WP_198024445.1	248	73.39%
R. taiwanensis LS-293^T	WP_132690711.1	246	75.82%
R. tropicus SCSIO 52909^T	WP_207957185.1	248	81.05%

3.1.3. PHA synthase

For the third and last enzyme, two separate PHA synthase (EC 2.3.1.304) classes: class I and class III, were searched and analyzed. In this approach, to complement the research and results obtained by Kouřilová et al. (2021), only the newly sequenced species were searched and presented in Table 3.3.

The class III PHA synthase, composed by two subunits coded by *phaC* and *phaE* genes, were initially found in all of the *Rubrobacter* species used in this analysis, with the complete genome available using BLAST. However, with the same methodology, the class I PHA synthase, composed by only one subunit coded by *phaC*, was not found, in the *R. calidifluminis* RG-1^T, *R. naiadicus* RG-3^T and *R. aplysinae* CECT 8425^T species. Although a phaC class I PHA synthase from *R. marinus* SCSIO 52915^T was found in Kouřilová et al. (2021) work, the protein accession Nº and the corresponding amino acid information was not available and was therefore not evaluated. It is also important to note that the *phaC* gene encoding class I PHA synthase is different from *phaC* gene class III PHA synthase.

Table 3.3. - PHA synthases (class I and class III) along with their constituent subunits, examined in the selected *Rubrobacter* species. The information was retrieved from the GenBank public database.

***Rubrobacter* species**	**PHA class**	**PHA subunit**	**Protein accession Nº**
R. aplysinae	Class I	phaC	n.d.
CECT 8425^{T}	Class III	phaC	WP_047865909.1
		phaE	WP_047865908.1
R. calidifluminis	Class I	phaC	n.d.
RG-1^{T}	Class III	phaC	WP_273841781.1
		phaE	WP_273841783.1
R. naiadicus	Class I	phaC	n.d.
RG-3^{T}	Class III	phaC	WP_273887813.1
		phaE	WP_273887814.1
R. radiotolerans	Class I	phaC	WP_038682553.1
DSM 5868^{T}	Class III	phaC	WP_038682548.1
		phaE	WP_198024477.1
R. taiwanensis	Class I	phaC	WP_132688328.1
LS-293^{T}	Class III	phaC	WP_132691807.1
		phaE	WP_207890443.1
R. xylanophilus	Class I	phaC	ABG05314.1
DSM 9941^{T}*	Class III	phaC	ABG05313.1
		phaE	ABG05312.1
R. radiotolerans	Class I	phaC	AHY47371.1
RSPS-4*	Class III	phaC	AHY47368.1
		phaE	AHY47367.1
R. indicoceani	Class I	phaC	WP_240432455.1
SCSIO 08198^{T}*	Class III	phaC	WP_119069243.1
		phaE	WP_205543964.1
R. tropicus	Class I	phaC	QIN85027.1
SCSIO 52909^{T}*	Class III	phaC	QIN82004.1
		phaE	QIN85028.1
R. marinus	Class I	phaC	n.a.
SCSIO 52915^{T}*	Class III	phaC	QIN79882.1
		phaE	QIN79881.1

n.a.: not available. n.d.: not detected. * Results from Kouřilová et al. (2021).

3.1.3.1. Lipase box-like in phaC

Since no prior research had explored the conserved regions of the *phaC* genes and their respective encoded protein in the *Rubrobacter* genus, this study was conducted to investigate whether these regions have any impact on the phenotypic outcomes. Several consensus lipase box-like sequences, required for phaC activity, were identified and

examined to better understand and compare the similarities between the various species selected. In this part, the *phaE* encoded protein was not addressed given the lack of information and knowledge of its function (Neoh et al., 2022), ensuring a greater focus on the most important subunits, *phaC* encoded protein class I and class III (Obruča et al., 2022).

Research results for the *Rubrobacter* PHA synthases conserved regions showed some differences between the amino acid sequences in the two enzymes, on both phaC class I and phaC class III. It was also found that there were differences even within the conserved motif of the phaC class I subunit.

First, in the phaC class I, beginning at position 352, the common conserved region, represented inside of the PHA-related lipase box-like, showed two different patterns, with the arrangement consisting in the respective order: Glycine-Tyrosine-Cysteine-(Isoleucine or Valine)-Glycine-Glycine pattern (G-Y-C-(I or V)-G-G) (Figure 3.1., A). *R. indicoceani* SCSIO 08198^T, *R. radiotolerans* DSM 5868^T, *R. radiotolerans* RSPS-4 and *R. xylanophilus* DSM 9941^T have an isoleucine amino acid residue. *R. taiwanensis* LS-293^T and *R. tropicus* SCSIO 52909^T have a valine amino acid residue. Although phaC class I PHA synthase from *R. marinus* SCSIO 52909^T was found in Kouřilová et al. (2021) work, the accession number of the protein and the corresponding amino acid information was not available and therefore this species was not evaluated in this part of the work.

For the phaC subunit class III, beginning at position 146, the common conserved region represented inside of a PHA-related lipase box-like has a pattern arrangement in the respective order: Glycine-Tyrosine-Cysteine-Methionine-Glycine-Glycine (G-Y-C-M-G-G) (Figure 3.1., B). This pattern is the same in all the *Rubrobacter* species with the phaC class III reported.

Full sequences alignments are represented in Figure 7.1. and Figure 7.2.

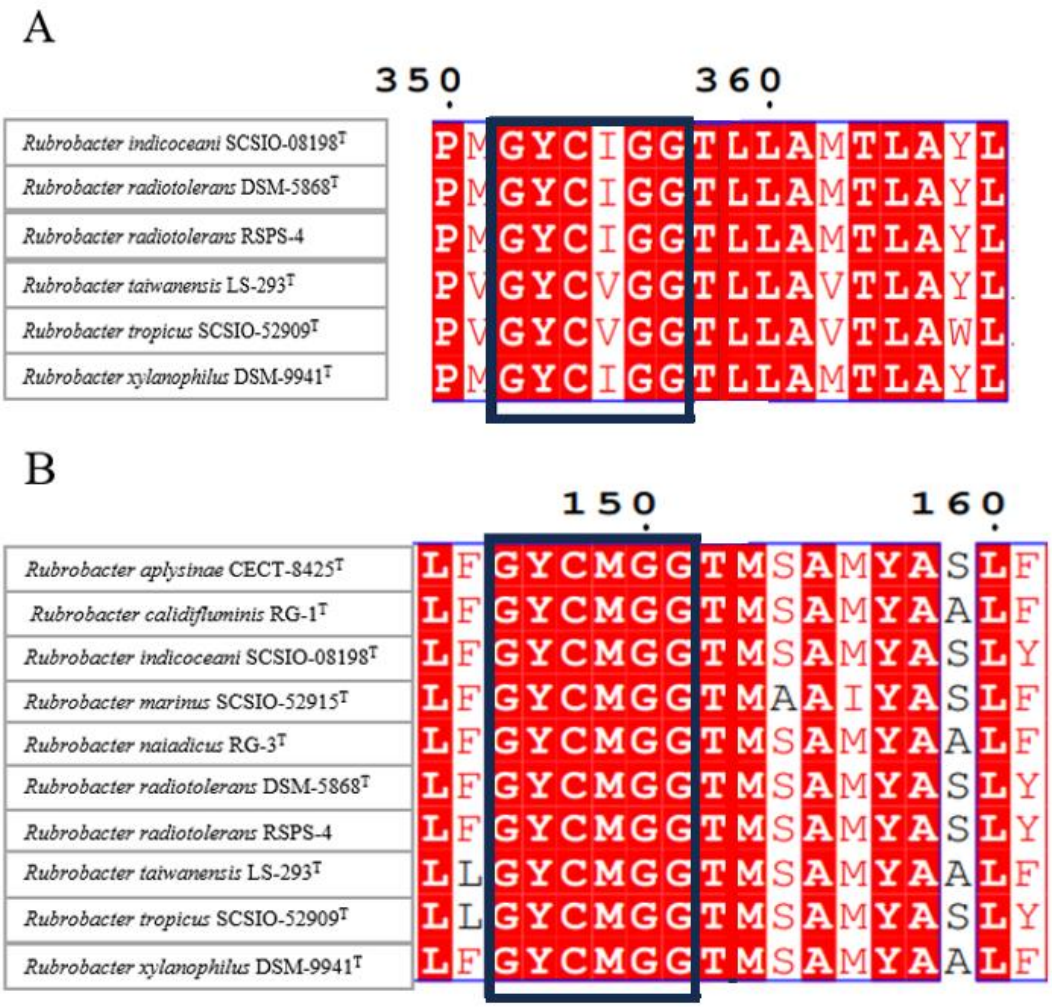

Figure 3.1. - Partial sequence alignment of the *phaC* encoded protein with the corresponding lipase box-like conserved region. A: phaC class I PHA synthetase subunit. B: phaC class III PHA synthetase subunit. All the sequences are related to the selected *Rubrobacter* species with reported phaC synthase subunit. The sequences were retrieved from the GenBank public database and aligned with the Clustal Omega tool within the MEGA11 software and visualized with the Espript 3.0. online tool.

3.2. Phenotypic analysis

3.2.1. Growth media conditions optimization

In this experiment, *R. xylanophilus* DSM 9941^T and *R. radiotolerans* DSM 5868^T were the selected species for growth media condition optimization. These cultures were cultivated in *Thermus* liquid medium supplemented with various tryptone and yeast extract concentrations (1 g/L, 2.5 g/L and 5 g/L) and Tryptic soy broth medium, at their optimal growth temperature and at 50ºC, over the course of 72 hours. The optical density growth curves were plotted and the specific growth rate was calculated.

In Figure 3.2., *R. radiotolerans* DSM 5868^{T} obtained a higher biomass growth in the Tryptic soy broth medium, with an absorbance value of 6.02, after 72 hours, at its optimum growth temperature of 45°C. However, the highest value recorded for specific growth rate was with *Thermus* medium with tryptone and yeast extract concentrations of 1 g/L, with a value of 0.0557 h^{-1}. Also, at the optimum growth temperature of 60ºC, *R. xylanophilus* DSM 9941^{T} produced a higher biomass after 72 hours in *Thermus* medium, with tryptone and yeast extract concentrations of 5 g/L, with a maximum absorbance value of 6.41. Here as well, the highest value recorded for the specific growth rate was with *Thermus* medium with tryptone and yeast extract concentrations of 1 g/L, with a value of 0.117 h^{-1}.

In the case of growth at a temperature of 50°C, both species underperformed compared with the growth at their optimal growth temperature, with both *R. xylanophilus* DSM 9941^{T} and *R. radiotolerans* DSM 5868^{T} obtaining higher biomass with *Thermus* medium, with tryptone and yeast extract concentrations of 1 g/L, obtaining absorbance values of 1.78 and 4.7, respectively. The highest specific growth rate obtained by *R. xylanophilus* DSM 9941^{T} and *R. radiotolerans* DSM 5868^{T} species, was also in the same medium conditions, where values of 0.086 h^{-1} and 0.028 h^{-1} were registered, respectively. The growth of the biomass of *R. radiotolerans* DSM 5868^{T} was minimal in *Thermus* medium with concentrations of tryptone and yeast extract of 5 g/L, at both temperatures. Under these specific conditions, it was not considered conducive to the continued growth of this species.

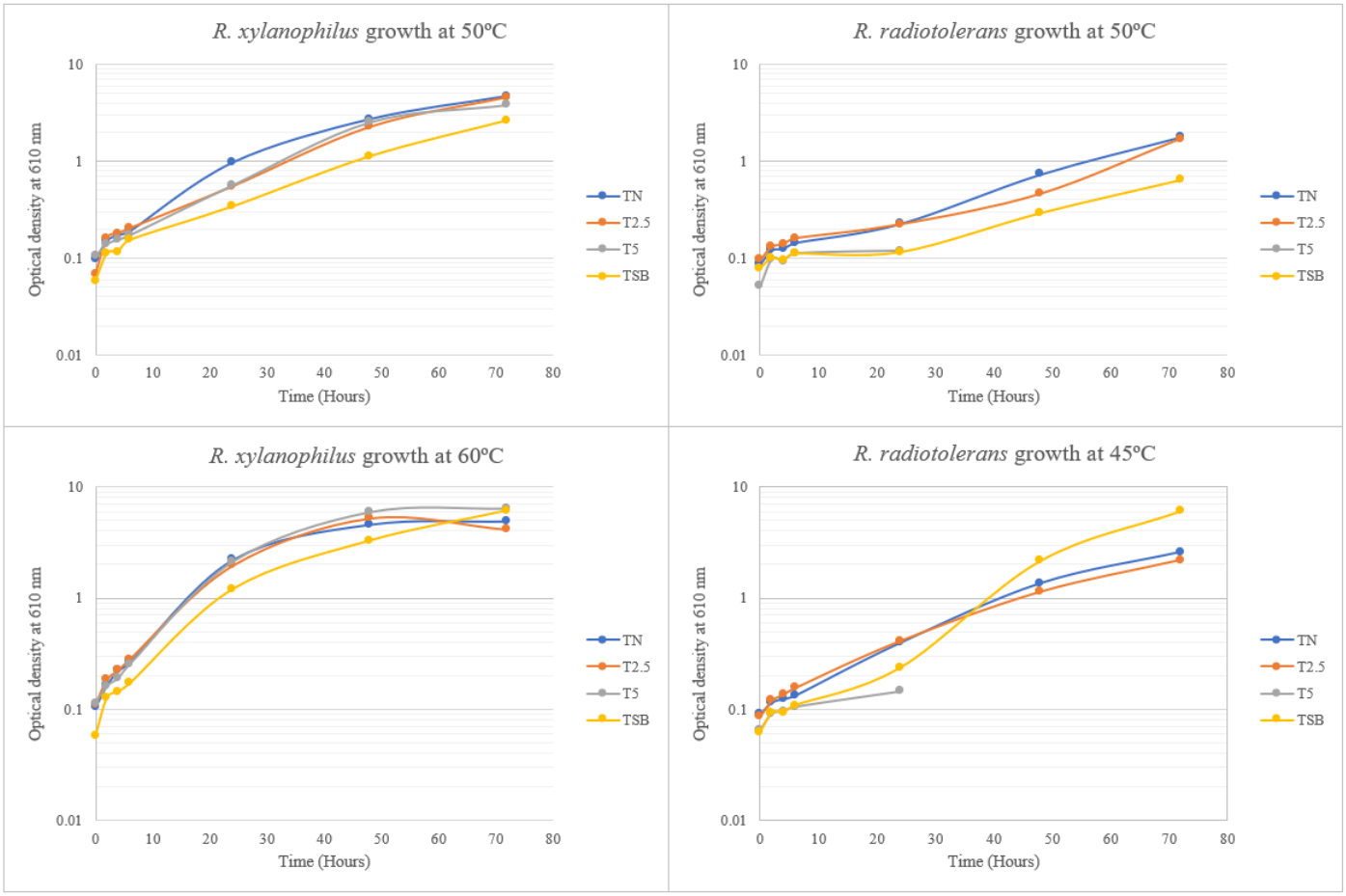

Figure 3.2. - *R. xylanophilus* DSM 9941^T and *R. radiotolerans* DSM 5868^T growth curves. TN: *Thermus* medium (tryptone and yeast extract concentrations of 1 g/L). T2.5: *Thermus* medium (tryptone and yeast extract concentrations of 2.5 g/L). T5: *Thermus* medium (tryptone and yeast extract concentrations of 5 g/L). TSB: Tryptic soy broth.

3.2.2. Biomass production

In this segment, biomass production results were presented according to the optimum growth temperature of the species, recorded at an optical density of 610 nm (Figure 3.3.).

In the case of mesophilic species, *R. bracarensis* CECT 7924^T growth was very tenuous, with a recorded optical density of 0.16. *R. aplysinae* CECT 8425^T growth was almost nonexistent after 120 hours of growth.

Moderate thermophilic species such as *R. radiotolerans*, strain DSM 5868^T and strain RSPS-4, obtained a higher value compared to the mesophilic species used in this study, obtaining an optical density value of 0.411 and 0.4, respectively, after 24 hours of growth. They also, respectively, obtained specific growth rate values of 0.0629 h^{-1} and 0.0508 h^{-1}.

Thermophilic species such as *R. xylanophilus* DSM 9941^{T}, *R. calidifluminis* RG-1^{T}, *R. naiadicus* RG-3^{T} and *R. taiwanensis* LS-293^{T}, obtained the highest optical density values, after 24 hours of growth, recording values of 2.215, 0.855, 0.835 and 0.887, respectively. The species that obtained the highest specific growth rate was *R. xylanophilus* DSM 9941^{T}, obtaining a value of 0.1219 h^{-1}. *R. calidifluminis* RG-1^{T}, *R. naiadicus* RG-3^{T} and *R. taiwanensis* LS-293^{T} species obtained a specific growth rate of 0.0843 h^{-1}, 0.0656 h^{-1} and 0.0836 h^{-1}, respectively.

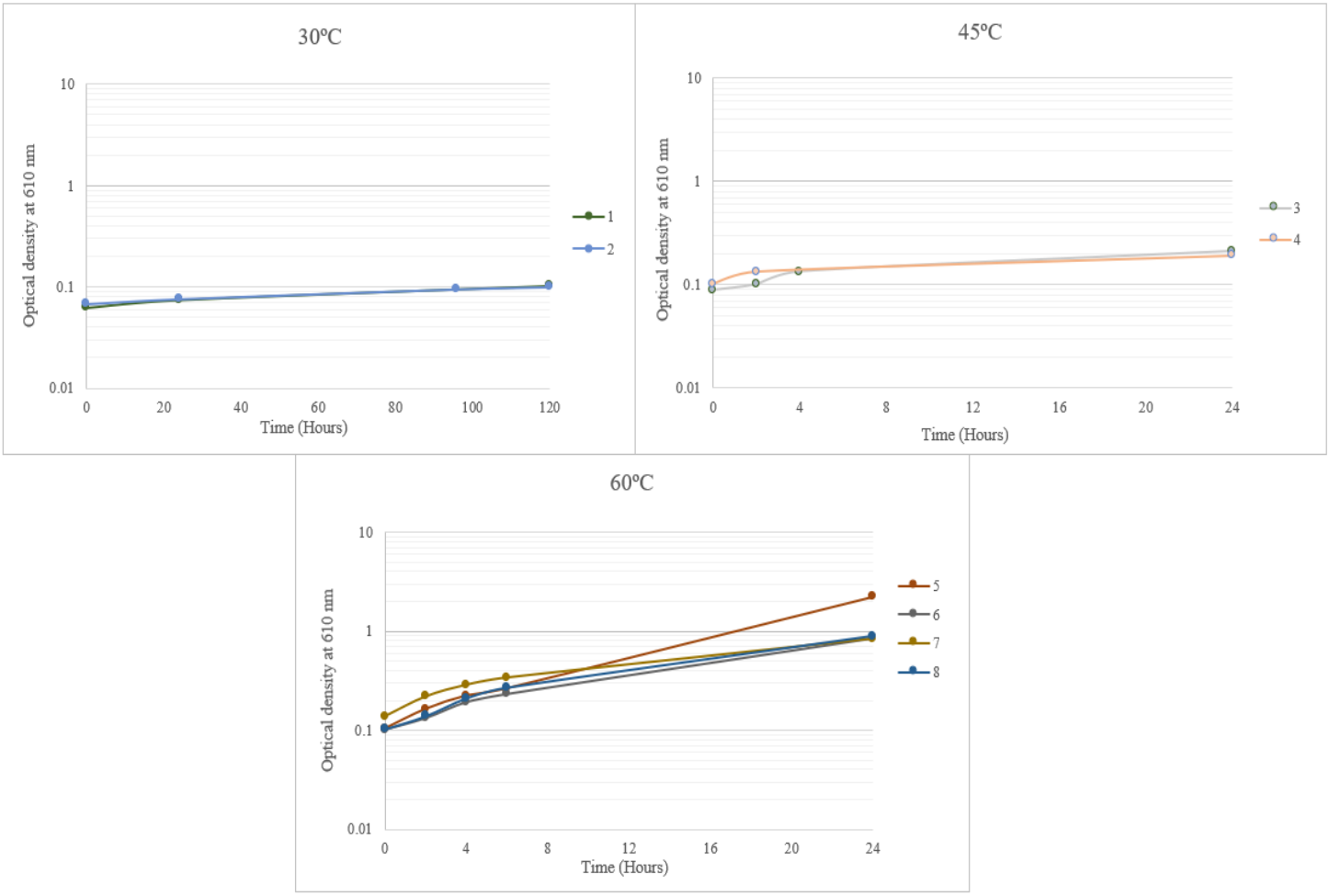

Figure 3.3. - Growth curves at the optimum growth temperature in *Thermus* medium. 1: *R. bracarensis* CECT 7924^{T}. 2: *R. aplysinae* CECT 8425^{T}. 3: *R. radiotolerans* DSM 5868^{T}. 4: *R. radiotolerans* RSPS-4. 293^{T}. 5: *R. xylanophilus* DSM 9941^{T}. 6: *R. calidifluminis* RG-1^{T}. 7: *R. naiadicus* RG-3^{T}. 8: *R. taiwanensis* LS-293^{T}.

3.2.3. Enhanced PHA accumulation

After biomass production characterization, enhancement of PHA accumulation of the cells on the various *Rubrobacter* species was then performed. Results are presented according to the optimum growth temperature of the species, recorded at an optical density of 610 nm (Figure 3.4.).

Here, no growth was done on MSM medium in the case of mesophilic species such as *R. bracarensis* CECT 7924^{T} and *R. aplysinae* CECT 8425^{T} due to the inherent challenges already associated with biomass production. In moderate thermophilic species *R. radiotolerans*, strains DSM 5868^{T} and RSPS-4, the optical density measured after 48 hours was 0.537 and 0.867 and specific growth rates of 0.049 h^{-1} and 0.0491 h^{-1}, respectively. In the thermophilic species such as *R. xylanophilus* DSM 9941^{T}, *R. calidifluminis* RG-1^{T}, *R. naiadicus* RG-3^{T} and *R. taiwanensis* LS-293^{T}, obtained here, as well, the highest optical density values after 48 hours of growth with enhanced PHA accumulation medium, with values of 2.05, 1.766, 1.962 and 0.978, respectively. In the same order, the specific growth rates obtained were 0.0682 h^{-1}, 0.0487 h^{-1}, 0.0523 h^{-1} and 0.0481 h^{-1}.

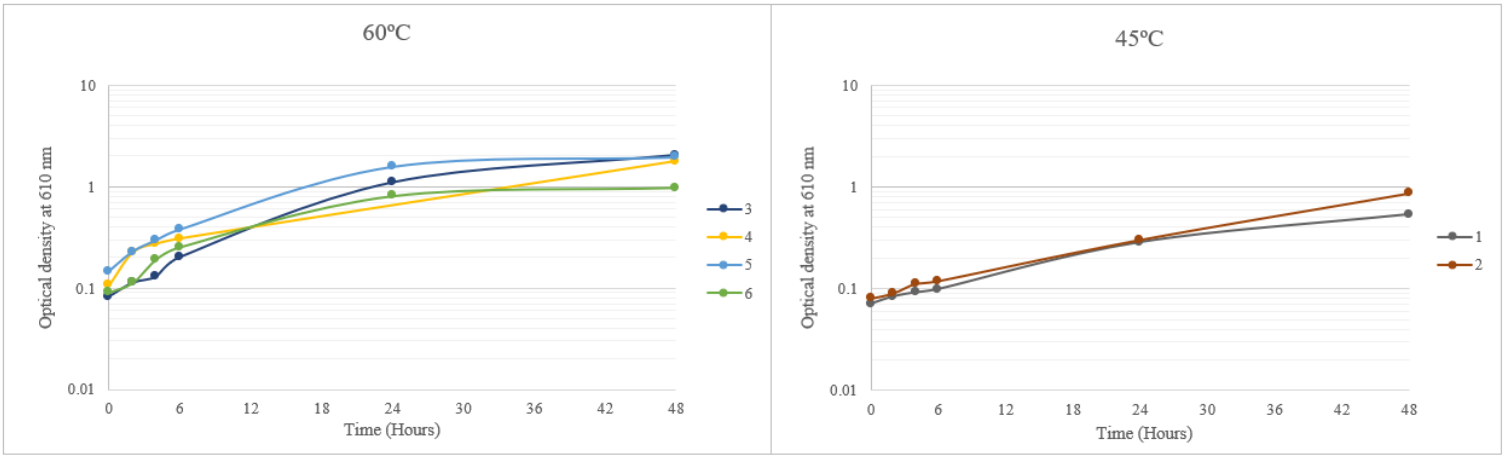

Figure 3.4. - *Rubrobacter* species growth curve in MSM supplemented with 2% glucose. 1: *R. radiotolerans* DSM 5868^{T}. 2: *R. radiotolerans* RSPS-4. 3: *R. xylanophilus* DSM 9941^{T}. 4: *R. calidifluminis* RG-1^{T}. 5: *R. naiadicus* RG-3^{T}. 6: *R. taiwanensis* LS-293^{T}.

3.2.4. Plate assay method for rapid detection of PHA accumulators

To obtain an initial visualization for potential PHA accumulation, a rapid screening assay was conducted by adapting a modified Sudan black B method. The *Rubrobacter* species used in this experiment were grown only in *Thermus* solid medium to first get an idea if there is actually an accumulation of PHA in the species without any PHA growth enhancement. In this experiment, *R. radiotolerans* RSPS-4, *R. calidifluminis* RG-1^{T}, *R.*

naiadicus RG-3^T and *R. xylanophilus* DSM 9941^T were the selected species to observe PHA accumulation. The colonies unable to incorporate the Sudan Black B stain were considered negative while PHA producers that retained the stain and appeared with a black tone were considered positive.

In Figure 3.5., image A, *R. radiotolerans* RSPS-4 effectively retained the Sudan black B stain, resulting in a distinctive black coloration of the colonies, after being rinsed with water and ethanol 96%. This black coloration served as a positive indicator of the presence of accumulated PHA. On the same plate, the negative control species used in this experiment, *E. coli* ATCC 29922, did not show the ability to retain the stain. This outcome granted a negative result in this species, indicating the absence of any accumulated PHA. On the second plate (Figure 3.5., image B) *R. calidifluminis* RG-1^T and *R. xylanophilus* DSM 9941^T appeared to be able to retain the Sudan Black B stain, meaning it has potential for PHA synthesis and consequently, accumulation. However, in this approach, the *R. naiadicus* RG-3^T species did not retain the Sudan Black B stain, granting it a negative result for PHA accumulation.

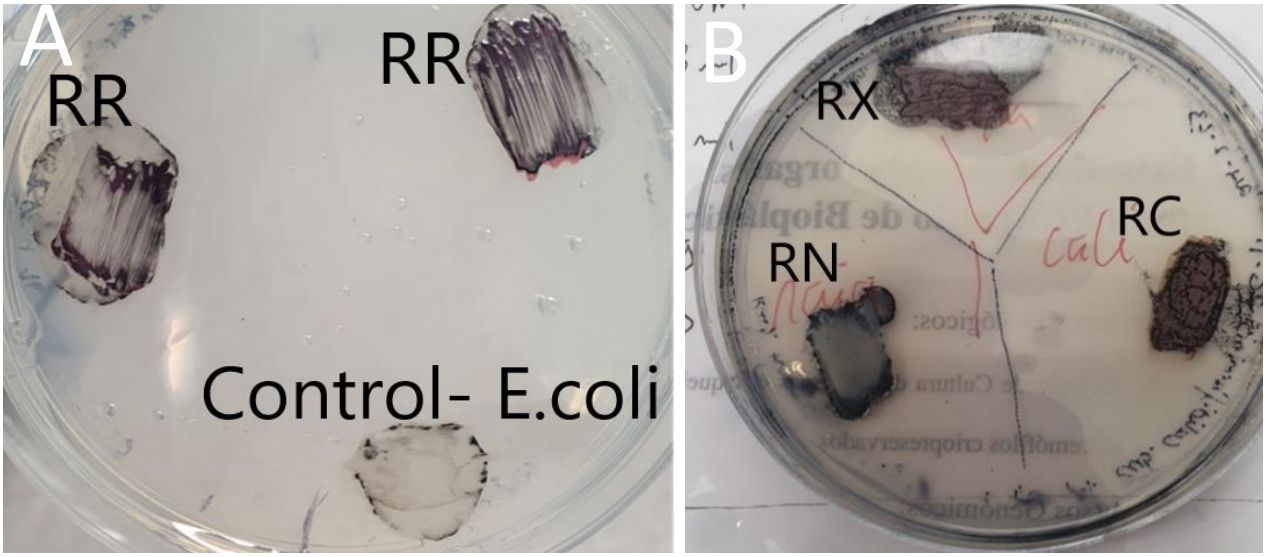

Figure 3.5. - Plate assay method for PHA production detection. A: RR: *R. radiotolerans* RSPS-4. Control - E. coli: *E. coli* ATCC 29922. B: RX: *R. xylanophilus* DSM 9941^T. RN: *R. naiadicus* RG-3^T. RC: *R. calidifluminis* RG-1^T.

3.2.5. Sudan black staining and optical microscopy

After using the modified Sudan Black B method, the normal procedure of this method was then performed. To confirm that PHA accumulation had occurred after growth in MSM for enhanced PHA production, the cells should show PHA inclusions

with a dark tone, between dark blue to black color range visualized by optical microscopy (Mesquita et al., 2015). All species present in Figure 3.6., were taken after 48 hours of growth on MSM, except for *R. bracarensis* CECT 7924^T and *R. aplysinae* CECT 8425^T, which were taken after 120 hours, in *Thermus* medium.

According to the results obtained by Sudan black B staining method and visualized by optical microscopy, *R. xylanophilus* DSM 9941^T, *R. radiotolerans* RSPS-4 and *R. radiotolerans* DSM 5868^T showed some visible dark tone granules, confirming preliminary an accumulation of PHA inside of the cells. *R. taiwanensis* LS-293^T appeared to have some dark inclusions but the result was inconclusive given the small size of the cells and, consequently, the difficult visualization of the granules. Inside the *R. bracarensis* CECT 7924^T cells, it was possible to visualize small dark granules in some cells. However, these inclusions were hard to observe as well. In the case of *R. calidifluminis* RG-1^T, *R. naiadicus* RG-3^T and *R. aplysinae* CECT 8425^T cells, it was not possible to detect any PHA granules.

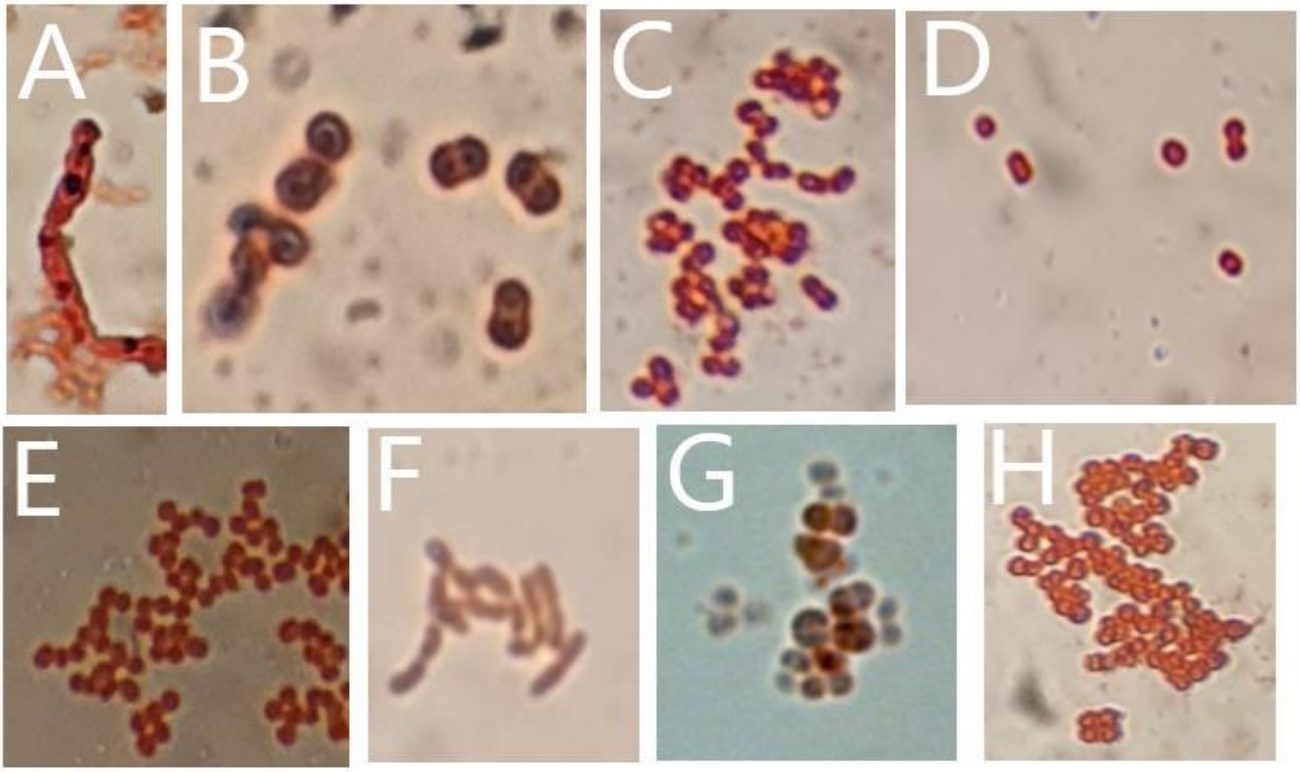

Figure 3.6. - *Rubrobacter* species selected for observation using the Sudan black B staining technique under an optical microscope (Carl Zeiss Axio Imager A2) with a 100x oil immersion objective. A: *R. xylanophilus* DSM 9941^T. B: *R. radiotolerans* RSPS-4. C: *R. radiotolerans* DSM 5868^T. D: *R. calidifluminis* RG-1^T. E: *R. naiadicus* RG-3^T. F: *R. taiwanensis* LS-293^T. G: *R. bracarensis* CECT 7924^T. H: *R. aplysinae* CECT 8425^T. A, B, C, D, E and F grown during 48 hours in MSM. G and H grown during 120 hours in *Thermus* medium.

3.2.6. Transmission electron microscopy

In order to enhance the visualization of the granules within the cells, TEM was conducted to verify the results achieved through optical microscopy, using the same species employed in the Sudan black B staining technique. The cells utilized in this experiment were examined after being cultured in MSM for 24 hours at their optimum growth temperature. Due to the unavailability of images during the 48 hours growth period in MSM, only the 24 hours observation data was considered (Figure 3.7.).

Positive results were obtained from the *R. xylanophilus* DSM 9941^T, *R. radiotolerans* RSPS-4 and *R. radiotolerans* DSM 5868^T cell samples. Both strains of *R. radiotolerans* exhibited easily observable PHA granules within their cells, where some granules reached a diameter of up to 200 nm. In contrast, the PHA granules within *R. xylanophilus* DSM 9941^T cells were less developed. Nonetheless, in this species, granules with a diameter of up to 200 nm were still detectable. The images obtained for *R. taiwanensis* LS-293^T were inconclusive as the cells did not show any visible PHA granules. In addition, the cells appeared to be lysed and some even fragmented. It was not possible to obtain the images for *R. calidifluminis* RG-1^T, *R. naiadicus* RG-3^T, *R. bracarensis* CECT 7924^T and *R. aplysinae* CECT 8425^T.

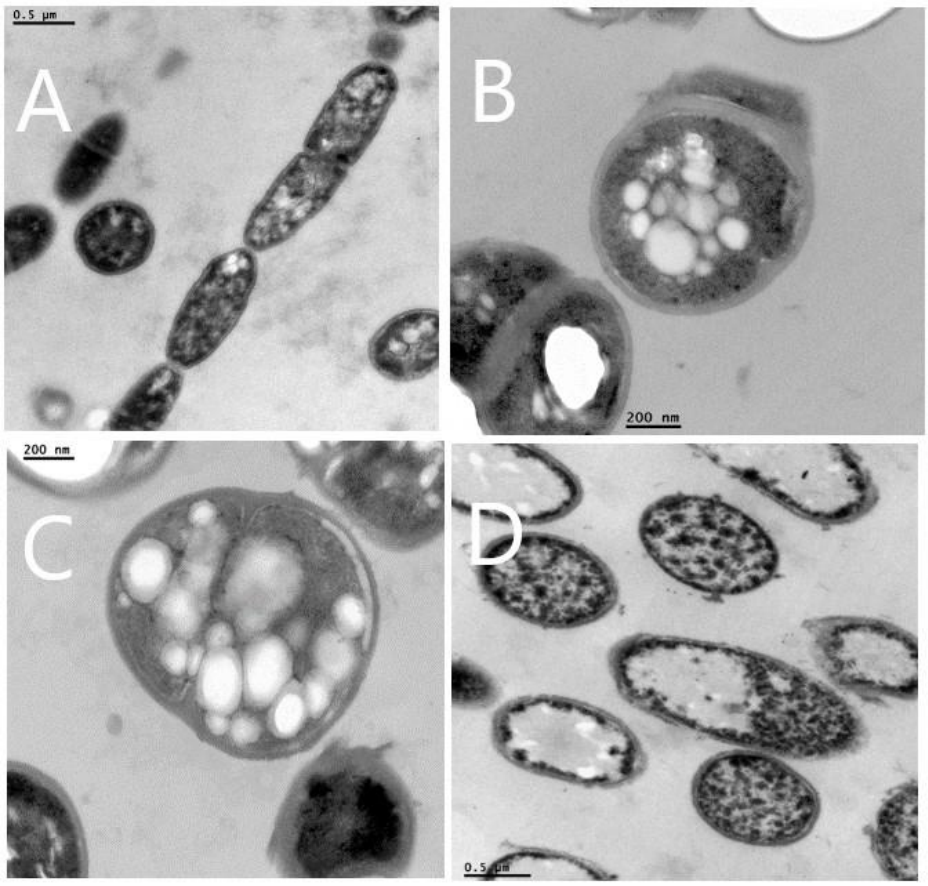

Figure 3.7. - *Rubrobacter* species selected for TEM observation. A: *R. xylanophilus* DSM 9941^T. B: *R. radiotolerans* RSPS-4. C: *R. radiotolerans* DSM 5868^T. D: *R. taiwanensis* LS-293^T. Cells were observed after cultivation in MSM, for 24 hours, at their optimal growth temperature.

3.2.7. Detection of PHA

Detection of PHA was performed using a method developed by Law and Slepecky (Law & Slepecky, 1961). Although the method is based on the quantification of PHA, in this work it was used only for their detection. In order to determine whether the produced substance of each species was PHA or not, the synthesized product underwent digestion using concentrated H_2SO_4 to convert it into crotonic acid. Afterward, the absorption spectrum obtained was measured within the 200 to 260 nm range, with the expected peak for PHA detection being at 235 nm and a graph was plotted (Figure 3.8.).

In this experiment, PHA detection was performed after 48 hours of cell cultivation in MSM at their optimal growth temperature, following the completion of the extraction process. *R. xylanophilus* DSM 9941^T, a species previously identified as a producer of PHA (Kouřilová et al., 2021), served as the positive control. The absorbance of this specie exhibited a peak at the wavelength of 235 nm, with a value reaching 1.92, which is within

the anticipated wavelength for the detection of PHA. This observation was supported by a graph showing the expected profile, confirming the presence of PHA accumulation in this species (Law & Slepecky, 1961). During the experiment, *E. coli* ATCC 29922, used as the negative control, displayed an absence of peaks and exhibited minimal levels of absorbance across the entire range of measurements used. It was observed that both strains of *R. radiotolerans* RSPS-4 and *R. radiotolerans* DSM 5868^T had absorbance peaks at 235 nm, with values of 1.079 and 0.667, respectively. Despite the graph profiles of both strains of *R. radiotolerans* not displaying as pronounced results as observed in *R. xylanophilus* DSM 9941^T, they were considered positive due to the presence of a peak detected at the expected wavelength. On the other hand, no peaks were registered in *R. calidifluminis* RG-1^T, *R. naiadicus* RG-3^T, *R. bracarensis* CECT 7924^T and *R. aplysinae* CECT 8425^T species and the graph profiles remained relatively flat across the entire wavelength range employed in this experiment, indicating a lack of significant PHA accumulation.

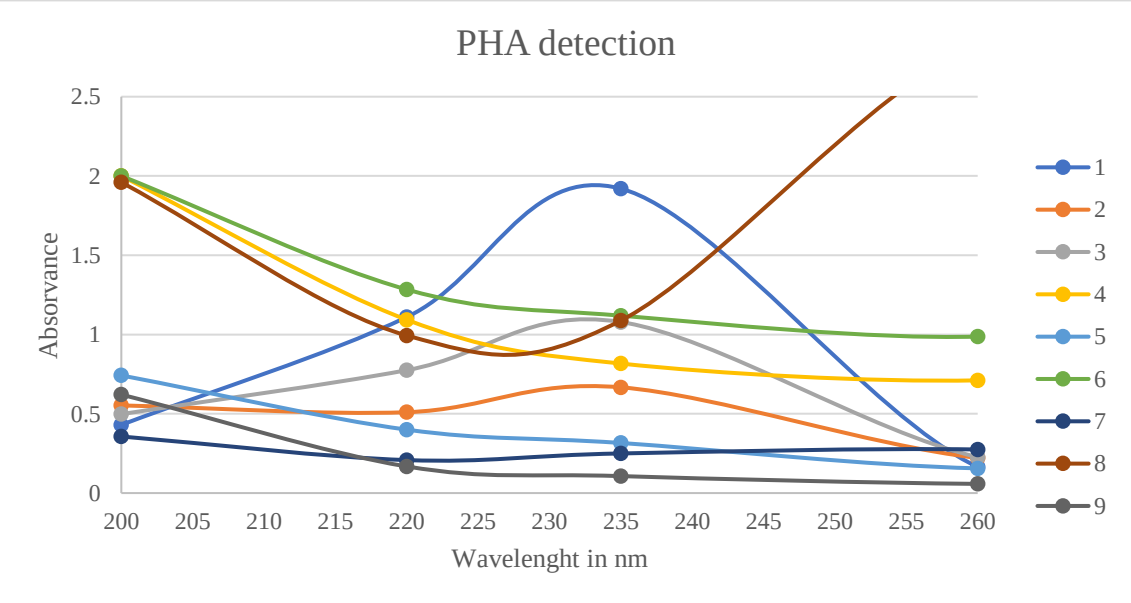

Figure 3.8. - Measurement of crotonic acid by absorbance between 200 nm and 260 nm of *Rubrobacter* species. 1: *R. xylanophilus* DSM 9941^T. 2: *R. radiotolerans* DSM 5868^T, 3: *R. radiotolerans* RSPS-4. 4: *R. taiwanensis* LS-293^T. 5: *R. calidifluminis* RG-1^T. 6: *R. naiadicus* RG-3^T. 7: *R. bracarensis* CECT 7924^T. 8: *R. aplysinae* CECT 8425^T. 9: *E. coli* ATCC 29922. 1, 2, 3, 4, 5 and 6 grown during 48 hours in MSM. 7 and 8 grown during 120 hours in *Thermus* medium. 9 grown during 24 hours in LB medium.

4. Discussion

PHA polymers are being extensively studied due to their numerous potential applications and highly promising characteristics. This increased attention is a response to the growing demand for eco-friendly and biodegradable alternatives to conventional petroleum-based plastics, driven by concerns about plastic pollution (Chamas et al., 2020). Despite being a minor player in the bioplastics market, comprising less than 2% of the total bioplastics produced in 2020, PHA future growth use are anticipated to be significant (Obruča et al., 2022). PHA accumulation has been already detected in many different species. However, the discovery for new PHA synthesizing species suitable for commercialization remains vital, focusing on the search for species capable of higher PHA yield at lower production cost (Albuquerque et al., 2007). Extremophile microorganisms, particularly halophilic and thermophilic species, have recently attracted interest for their efficient PHA production potential (Obruča et al., 2022). Recently, two thermophilic species, *R. spartanus* DSM 102139^{T} and *R. xylanophilus* DSM 9941^{T}, proved their ability to produce this polymer (Kouřilová et al., 2021). However, in this experiment, in which these two species were tested phenotypically, only *R. xylanophilus* DSM 9941^{T} had its genome fully sequenced. Within this species, genes for two PHA synthase types were discovered: one for class I PHA synthetase (*phaC*) and another two for class III PHA synthetase (*phaC* and *phaE*) (Kouřilová et al., 2021; Obruča et al., 2022). This result is intriguing since, in thermophilic microorganisms, PHA biosynthesis is still poorly known or not as common as in halophilic microorganisms, as already mentioned previously (Obruča et al., 2022).

In this dissertation, a larger number of *Rubrobacter* species were analyzed to see if this synthesis is typical of this genus, exploring the genes and enzymes responsible for PHA production through genotypic analysis and consequently through phenotypic analysis. Table 4.1. summarizes the results obtained in this work.

The presence of *phaA* and *phaB* genes responsible for encoding phaA and phaB enzymes in all of the *Rubrobacter* species studied with the complete genome sequenced means that the species of this genus possess the capacity and machinery to synthesize PHA. Furthermore, the results suggest that *Rubrobacter* species exhibit substantial similarity in their phaA and phaB amino acid sequences. This similarity leads to the prediction that if one species possesses these genes and has demonstrated PHA production, as previously shown by Kouřilová et al. (2021), then it is likely that the other species also possess the capacity to synthesize PHA.

Table 4.1. - Summary of the study results.

***Rubrobacter* species**	**phaA**	**phaB**	**Class I PHA synthase**	**Class III PHA synthase**	**PHA accumulation**
R. aplysinae CECT 8425^T	+	+	-	+	-
R. calidifluminis RG-1^T	+	+	-	+	-
R. indicoceani SCSIO 08198^T	+	+	+*	+*	n.a.
R. marinus SCSIO 52909^T	+	+	+*	+*	n.a.
R. naiadicus RG-3^T	+	+	-	+	-
R. radiotolerans DSM 5868^T	+	+	+	+	+
R. radiotolerans RSPS-4	+	+	+*	+*	+
R. taiwanensis LS-293^T	+	+	+	+	-
R. tropicus SCSIO 52915^T	+	+	+*	+*	n.a.
R. xylanophilus DSM 9941^T	+	+	+*	+*	+**

n.a.: not assessed. +: detected. -: not detected. * Results from Kouřilová et al. (2021). ** Results from Kouřilová et al. (2021) and replicated in this work.

Additionally, as part of this study, a comparative analysis was conducted on the two classes of PHA synthetase. The investigation revealed a significant observation: different *Rubrobacter* species may exhibit variations in the presence or absence of specific PHA synthetase classes, as the class I PHA synthetase, encoded by only one unit of *phaC* gene, was not found in this study, in the *R. calidifluminis* RG-1^T, *R. naiadicus* RG-3^T and *R. aplysinae* CECT 8425^T species, unlike class III PHA synthase, encoded by only one unit of *phaC* gene and another unit of *phaE* gene, which was found in all species studied. This result suggests a diversification in the mechanisms and potential for PHA synthesis among these extremophile organisms. Such insights are crucial for understanding the diversity and complexity of PHA metabolic pathways in *Rubrobacter* species and can pave the way for further investigations into the genetic factors in this process. In addition, a problem was found during the search of genes in the genomes using the BLAST tool. The class III phaE subunit (accession Nº: SMC06735.1), in the case of the *R. radiotolerans* DSM 5868^T species, is sometimes connoted as a phaR However, as already mentioned in the work carried out by Kouřilová et al. (2021), there is a significant homology between the phaE and phaR subunits. The presence of the identified phaR in this species may potentially be attributed to an annotation error. However, if it indeed exists, it would suggest the presence of a class IV PHA synthetase, typically constituted

by a phaC subunit and a phaR subunit, instead of a class III PHA synthase. Further research is required to elucidate this matter conclusively.

Given the variances in these species, a detailed analysis was also made regarding the conserved regions, in this case, the lipase box-like of the phaC amino acid sequences of the PHA synthases. These regions are important for the function of the enzyme active site, critical to the polymer elongation process in many species that synthesize PHA (Thomas et al., 2020). The lipase box-like sequence of the phaC subunit is usually organized in this conserved order: Glycine-X-Cysteine-X-Glycine-Glycine (G-X-C-X-G-G), where X can be any amino acid, depending on the nature of the PHA-producing species (Thomas et al., 2020).

In this work, the PHA-related lipase box-like of the several *Rubrobacter* species studied showed two distinct patterns with the arrangement consisting in the respective order: Glycine-Tyrosine-Cysteine-(Isoleucine or Valine)-Glycine-Glycine pattern (G-Y-C-(I or V)-G-G), in the phaC class I PHA synthase. To the best of my knowledge, this specific pattern is not present in other species in published studies where the PHA-related lipase box-like were searched. However, using the BLAST tool, it was possible to identify other species with the same patterns. First, in the case of the (G-Y-C-V-G-G) motif, the halophilic *Nitratireductor* genus (Marasco et al., 2023), has this lipase box-like in its class I PHA synthetase, as in *Nitratireductor aquibiodomus* (accession Nº: WP_007008219.1), in *Nitratireductor rhodophyticola* (accession Nº WP_223003919.1) and in *Nitratireductor pacificus* (accession Nº: WP_008595969.1). Unfortunately, it should be noted that while the genetic machinery for PHA synthesis was detected within the *Nitratireductor* genus, the actual production of PHA has not yet been tested (Marasco et al., 2023). On the other hand, the (G-Y-C-I-G-G) motif is found, for example in the class I PHA synthetase from an unclassified *Gammaproteobacteria bacterium* (accession Nº: MCP4125952.1), but as in the previous pattern, PHA synthesis has not yet been detected (Sruamsiri et al., 2020).

For the phaC class III PHA synthase lipase box-like, the pattern arrangement is in the respective order: Glycine-Tyrosine-Cysteine-Methionine-Glycine-Glycine (G-Y-C-M-G-G) in all the *Rubrobacter* species studied. This pattern is reported in species such as the halophilic *Haloferax mediterranei* ATCC 33500^{T}, where the PHA accumulation is experimentally proven (Cui et al., 2017). Based on these results, there is evidence that it is possible to find PHA production in the various *Rubrobacter* species.

After the bioinformatics analysis, the synthesis of PHA in the selected *Rubrobacter* species was then tested experimentally. However, to verify what would be the best conditions to grow the bacteria, an optimization of the growth conditions was done. This involved the selection of various temperatures and culture media to determine the most suitable combination. *R. xylanophilus* DSM 9941^T and *R. radiotolerans* DSM 5868^T were the species selected for this experiment. It was found that, as expected, there was more biomass accumulation at their optimum growth temperature compared with the stipulated 50ºC growth temperature. In the case of the medium, although after 48 hours, at the optimum growth temperature, Tryptic soy broth provided higher values for biomass accumulation in these two species, *Thermus* medium with tryptone and yeast extract concentrations of 1 g/L, provided higher specific growth rate values. Given this result, this condition was chosen to standardize the conditions and used for the other *Rubrobacter* species.

In the biomass growth experiments, the growth of *R. xylanophilus* DSM 9941^T was much higher than the other *Rubrobacter* species. This suggests that there might be a factor favoring its growth beyond what is reported in the literature. One hypothesis is that the medium used may be more conducive to the growth of *R. xylanophilus* DSM 9941^T compared to other species. So, choosing and optimizing the medium for each specific species could lead to better growth results. In the case of *R. aplysinae* CECT 8425^T and *R. bracarensis* CECT 7924^T, biomass growth was very tenuous. However, it is also expected given that based on the literature description of these species, there is only a satisfactory growth after 168 to 360 hours of incubation, in the case of *R. aplysinae* CECT 8425^T (Kämpfer et al., 2014) and up to 720 hours, for *R. bracarensis* CECT 7924^T (Jurado et al., 2012). In this case, the growing time should have been extended more for these two species.

In the case of growth in MSM for enhanced PHA accumulation, it was anticipated from the outset that mesophilic *Rubrobacter* species would have great difficulty in achieving any growth. Growth on this medium was tried anyway, but after several failed attempts, the idea of growing on this medium was discarded. A potential explanation for this outcome could be the highly restricted growth specificity of these species, as they demand very precise conditions and a specific medium to achieve substantial growth (Jurado et al., 2012; Kämpfer et al., 2014). Thermophilic species such as *R. xylanophilus* DSM 9941^T, *R. calidifluminis* RG-1^T, *R. naiadicus* RG-3^T and *R. taiwanensis* LS-293^T, had the highest biomass growth, compared with the moderate thermophilic species *R.*

radiotolerans DSM 5868^T and *R. radiotolerans* RSPS-4. Some of these species originate from hot springs (*R. calidifluminis* RG-1^T, *R. naiadicus* RG-3^T, *R. taiwanensis* LS-293^T and *R. radiotolerans* RSPS-4), known for high concentrations of specific minerals. The similarity of the MSM composition to its natural habitat probably contributes to some of these species thriving in this environment (Chen et al., 2004; Selvarajan et al., 2018). With the growth in MSM it leaded to expected PHA accumulation within the cells, ready for further detailed analysis.

A straightforward PHA accumulation screening method was used to test several *Rubrobacter* species grown only in *Thermus* solid medium to get an initial idea of the actual accumulation of PHA in the species without any PHA growth enhancement conditions. PHA accumulation was confirmed in the duplicate samples of the *R. radiotolerans* RSPS-4, in *R. calidifluminis* RG-1^T and in *R. xylanophilus* DSM 9941^T. *R. naiadicus* RG-3^T did not retain Sudan black B. This experiment was not employed for other species, as it was determined that the results obtained in this assay were highly subjective, which could lead to false positives and false negatives.

Following cell growth in MSM, the conventional Sudan Black B method was subsequently employed in all *Rubrobacter* species to obtain a more comprehensive assessment of PHA accumulation within this genus. Here, *R. xylanophilus* DSM 9941^T, *R. radiotolerans* RSPS-4 and *R. radiotolerans* DSM 5868^T exhibited positive result, with clear accumulation of PHA within the cells. Visualizing the PHA granules in *R. taiwanensis* LS-293^T and *R. bracarensis* CECT 7924^T proved to be extremely challenging, to the extent that it was impossible to determine whether the black inclusions within the cells were PHA granules. In the case of *R. calidifluminis* RG-1^T, *R. naiadicus* RG-3^T and *R. aplysinae* CECT 8425^T, it was not possible to visualize any PHA granules.

Something that was also noticed in these experiments was that it was also possible to observe small dark inclusions in some *Rubrobacter* species, namely *R. xylanophilus* DSM 9941^T and *R. radiotolerans* RSPS-4 cells, after growth in *Thermus* medium. This means that although the recommended medium for PHA accumulation, MSM, was used, it is also very likely that just using the normal growth medium (without the use of any stress inducing factor) is sufficient to achieve PHA accumulation, as observed in the quick plate assay method. As said earlier, PHA-producing species are often divided into two groups depending on the culture conditions adaptability (Shahid et al., 2021). One hypothesizes that there is a possibility that at least some of the species in the genus *Rubrobacter* fall into the group of species where no limitations in nutrition are required

to promote PHA accumulation, in other words, PHA can be stored by the microbes during normal growth without any stimulus condition to enhance PHA accumulation.

The TEM methodology was performed to improve the visibility of the granules, present within the cells. This technique was employed to validate the results obtained from optical microscopy, using the very same species used in the Sudan black B staining method. In the case of *R. xylanophilus* DSM 9941^T, the results were not impressive as PHA granules were expected to be very prominent within the cells as visualized in the work of Kouřilová et al. (2021). This may have happened because of two reasons: The time of initiation of the fixation protocol that stops and preserves all metabolic processes of the microorganism as close as possible to the living state through the subsequent processing and imaging steps (Gallion et al., 2020), may have not go properly as there was an unknown experimental error which has caused the cells to continue with the metabolic process and consequently depolymerize the PHA, present within the cells. The other reason may simply be that the cells did not have the opportunity to form PHA in a greater amount, within the cells, at the time of the fixation procedure. In the case of the two strains of the species *R. radiotolerans*, the PHA granules were clearly identified. Since this species has never been tested for PHA synthesis, this result is a novelty, thus proving that PHA production exists in this *Rubrobacter* species. Finally, in the case of TEM images obtained for the species *R. taiwanensis* LS-293^T, no PHA accumulation could be verified. Furthermore, based on the observation of these cells, some were found to be lysed. This means that the sample sent to the microscopy facility was not in the best condition due to some experimental problem in sample preparation through the fixation protocol. In the case of the remaining species, *R. calidifluminis* RG-1^T, *R. naiadicus* RG-3^T, *R. bracarensis* CECT 7924^T and *R. aplysinae* CECT 8425^T, at the time of writing the thesis, it was not possible to obtain the TEM images, thus preventing checking if there was PHA accumulation in these species.

Given these results obtained and time constraints to optimize fixation conditions for TEM, it was necessary to resort to a PHA detection method to realize if the inclusions observed corresponded to PHA granules, corroborating the results obtained previously. A technique used for PHA detection was created by Law and Slepecky (1961). Although the approach is based on the quantification of PHA, this method has also been used only for its detection (Singh et al., 2019). The positive control, *R. xylanophilus* DSM 9941^T, demonstrated a clear peak at 235 nm, indicating the accumulation of PHA. This result correlates with a previous report done about the PHA accumulation in this species

(Kouřilová et al., 2021), confirming that *R. xylanophilus* DSM 9941^T is indeed a producer of PHA. The graph Figure 3.8. showed the expected profile which added credibility to the results and validated the accuracy of the experimental setup (Law & Slepecky, 1961). The negative control, *E. coli* ATCC 29922, showed an absence of peaks and minimal levels of absorbance across the entire wavelength range measured. This result demonstrates the specificity of the experimental approach, indicating that the absence of peaks in other bacterial strains is not a result of non-specific interactions or "background noise". The use of *E. coli* ATCC 29922 as a negative control also added strength to the experiment as it is a well-characterized bacteria with a known lack of PHA production (Wang et al., 2009). Both strains of *R. radiotolerans* (RSPS-4 and DSM 5868^T) showed a peak at 235 nm. Although the peak intensities were not as pronounced as observed in *R. xylanophilus* DSM 9941^T, the presence of a peak at the expected wavelength indicates accumulation of PHA in these strains, though possibly at lower levels compared to *R. xylanophilus* DSM 9941^T. For the *R. calidifluminis* RG-1^T, *R. naiadicus* RG-3^T, *R. bracarensis* CECT 7924^T and *R. aplysinae* CECT 8425^T, no peaks were registered, suggesting a lack of significant PHA accumulation in these bacterial strains, at least under the conditions of the experiment. This information provides valuable insights into the diversity of PHA production capabilities among different *Rubrobacter* species and it suggests that these last four particular strains may not be promising candidates for PHA production in the conditions tested.

The results from the genomic analysis and the phenotypic experiments made it possible to discuss and realize how the genomic differences observed can potentially influence PHA production. Since both strains, RSPS-4 and DSM 5868^T, of the *R. radiotolerans* species and the *R. xylanophilus* DSM 9941^T species were the only ones, under the conditions used in this study, to accumulate PHA, it was necessary to review the results of the genotype part to understand if there is any impact concerning the presence of different PHA synthetase classes in the genomes of the species. It was possible to observe that the species that obtained positive results for PHA accumulation also had the class I PHA synthase. Furthermore, within the phaC class I PHA synthase conserved area, these three strains that were positive for PHA accumulation were those that contained the same Glycine-Tyrosine-Cysteine-Isoleucine-Glycine-Glycine motif, unlike the other species which contained the arrangement Glycine-Tyrosine-Cysteine-Valine-Glycine-Glycine motif (except *R. indicoceani* SCSIO 08198^T which also had the pattern of those that tested positive but was not tested experimentally in this study). It can

be preliminarily said that having this motif, might result in a variation in catalytic activity and ultimately affect the yield of polymer synthesis. Nonetheless, further research is essential to elucidate the impacts of each pattern on the enzymes and to understand how the presence of PHA synthase class I might affect the synthesis capacity in the various species.

5. Conclusion and future work

This work has demonstrated that the species of the *Rubrobacter* genus have the molecular machinery potential to synthesize PHA since the *phaA* and *phaB* genes were present in all the species studied. However, in the case of the *phaC* genes, more specifically, the class I PHA synthase encoded by only one unit of *phaC* gene was only found in *R. radiotolerans* DSM 5868^T, *R. radiotolerans* RSPS-4, *R. taiwanensis* LS-293^T and *R. xylanophilus* DSM 9941^T species. Even within the conserved lipase box-like motif of the phaC class I PHA synthase, several variations appeared. *R. indicoceani* SCSIO 08198^T, *R. radiotolerans* DSM 5868^T, *R. radiotolerans* RSPS-4 and *R. xylanophilus* DSM 9941^T have an isoleucine amino acid residue and *R. taiwanensis* LS-293^T and *R. tropicus* SCSIO 52909^T have a valine amino acid residue.

In the phenotypic approach, it was found that *Thermus* medium was the most suitable for biomass growth and was used to normalize the conditions of the experiment. Then, potentiation of PHA accumulation in the mineral medium was done, supplemented with glucose as a carbon source. Using the Sudan Black B method for all species grown in the MSM, only the species *R. xylanophilus* DSM 9941^T, *R. radiotolerans* RSPS-4 and *R. radiotolerans* DSM 5868^T were verified with clarity, PHA accumulation. Then, to corroborate this result, with both TEM and the indirect PHA detection method, this accumulation was confirmed, which means that, through the growth conditions used in this work, *R. xylanophilus* DSM 9941^T, *R. radiotolerans* RSPS-4 and *R. radiotolerans* DSM 5868^T indeed can accumulate PHA.

In conclusion, the results obtained from the genomic and the phenotypic analyses suggest that the presence of the class I PHA synthetase with the isoleucine amino acid residue in the conserved region is related to PHA production in *Rubrobacter* species. This result reinforces the relationship between the existence of PHA synthase and successful PHA accumulation.

For future works, it is necessary to surpass the challenges regarding the lack of accumulation of PHA in some species as it may be due to not using optimal conditions, as experimentally approached or may be due to differences in the lipase box-like motif which impacts the capability to synthesize PHA in each particular species. In order to overcome this, the best means of boosting biomass growth and enhancing PHA accumulation, considering the best-suited medium and parameters, for each specific species, will have to be studied and optimized in more detail. Also, a broader search of

the type of motif linked to PHA synthesis that could have any impact on the accumulation of the PHA should be assessed.

For a detailed characterization of the PHA synthesized by each species, it is necessary to use techniques such as GS-MS and FT-IR to understand what type of PHA monomer is synthesized. Subsequently, it becomes possible to investigate the potential enhancement of the synthesized monomers by incorporating them into copolymers to have particular properties, including increased flexibility, thermal stability or biodegradability, improving the product in question for the various areas in the scientific field. Also, based on the yield of PHA synthesis, an economic study needs to be done to understand if this species has the potential to be used commercially, based on production costs, type of PHA synthesized and viability in the market (Możejko-Ciesielska & Kiewisz, 2016; Rehakova et al., 2023).

6. Bibliography

Aguirre-Ezkauriatza, E. J., Aguilar-Yáñez, J. M., Ramírez-Medrano, A., & Alvarez, M. M. (2010). Production of probiotic biomass (*Lactobacillus casei*) in goat milk whey: Comparison of batch, continuous and fed-batch cultures. *Bioresource Technology*, *101*(8), 2837–2844. https://doi.org/10.1016/J.BIORTECH.2009.10.047

Albuquerque, L., Johnson, M. M., Schumann, P., Rainey, F. A., & da Costa, M. S. (2014). Description of two new thermophilic species of the genus *Rubrobacter*, *Rubrobacter calidifluminis* sp. nov. and *Rubrobacter naiadicus* sp. nov., and emended description of the genus *Rubrobacter* and the species *Rubrobacter bracarensis*. *Systematic and Applied Microbiology*, *37*(4), 235–243. https://doi.org/10.1016/J.SYAPM.2014.03.001

Albuquerque, M. G. E., Eiroa, M., Torres, C., Nunes, B. R., & Reis, M. A. M. (2007). Strategies for the development of a side stream process for polyhydroxyalkanoate (PHA) production from sugar cane molasses. *Journal of Biotechnology*, *130*(4), 411–421. https://doi.org/10.1016/J.JBIOTEC.2007.05.011

Alcântara, J. M. G., Distante, F., Storti, G., Moscatelli, D., Morbidelli, M., & Sponchioni, M. (2020). Current trends in the production of biodegradable bioplastics: The case of polyhydroxyalkanoates. *Biotechnology Advances*, *42*, 107582. https://doi.org/10.1016/J.BIOTECHADV.2020.107582

Appiah-Otoo, I. (2022). Russia–Ukraine War and US Oil Prices. *Energy RESEARCH LETTERS*, *4*(Early View). https://doi.org/10.46557/001C.37691

Atiwesh, G., Mikhael, A., Parrish, C. C., Banoub, J., & Le, T. A. T. (2021). Environmental impact of bioplastic use: A review. *Heliyon*, *7*(9), e07918. https://doi.org/10.1016/J.HELIYON.2021.E07918

Bagchi, B., & Paul, B. (2023). Effects of crude oil price shocks on stock markets and currency exchange rates in the context of Russia-Ukraine conflict: Evidence from G7 Countries. *Journal of Risk and Financial Management*, *16*(2), 64. https://doi.org/10.3390/JRFM16020064

Basumatary, I. B., Mukherjee, A., Katiyar, V., & Kumar, S. (2020). Biopolymer-based nanocomposite films and coatings: recent advances in shelf-life improvement of fruits and vegetables. *Critical Reviews in Food Science and Nutrition*, *62*(7), 1912–1935. https://doi.org/10.1080/10408398.2020.1848789

Bedade, D. K., Edson, C. B., & Gross, R. A. (2021). Emergent approaches to efficient and sustainable polyhydroxyalkanoate production. *Molecules 2021*, *26*(11), 3463. https://doi.org/10.3390/MOLECULES26113463

Benson, D. A., Cavanaugh, M., Clark, K., Karsch-Mizrachi, I., Lipman, D. J., Ostell, J., & Sayers, E. W. (2012). GenBank. *Nucleic acids research*, *41*(1), 36-42. https://doi.org/10.1093/nar/gks1195

Bhola, S., Arora, K., Kulshrestha, S., Mehariya, S., Bhatia, R. K., Kaur, P., & Kumar, P. (2021). Established and emerging producers of PHA: Redefining the possibility.

Applied Biochemistry and Biotechnology, 193, 3812-3854. https://doi.org/10.1007/s12010-021-03626-5

Bhuwal, A. K., Singh, G., Aggarwal, N. K., Goyal, V., & Yadav, A. (2013). Isolation and screening of polyhydroxyalkanoates producing bacteria from pulp, paper, and cardboard industry wastes. *International Journal of Biomaterials, 2013*. https://doi.org/10.1155/2013/752821

Bugnicourt, E., Cinelli, P., Lazzeri, A., & Alvarez, V. A. (2014). Polyhydroxyalkanoate (PHA): Review of synthesis, characteristics, processing and potential applications in packaging. *Polymer Letters*, *8*, 791–808. http://doi.org/10.3144/expresspolymlett.2014.82

Carreto, L., Moore, E., Nobre, M. F., Wait, R., Riley, P. W., Sharp, R. J., & da Costa, M. S. (1996). *Rubrobacter xylanophilus* sp. nov., a new thermophilic species isolated from a thermally polluted effluent. *International Journal of Systematic and Evolutionary Microbiology*, *46*(2), 460-465. https://doi.org/10.1099/00207713-46-2-460

Castro, J. F., Nouioui, I., Asenjo, J. A., Andrews, B., Bull, A. T., & Goodfellow, M. (2019). New genus-specific primers for PCR identification of *Rubrobacter* strains. *Antonie van Leeuwenhoek, 112*, 1863-1874. https://doi.org/10.1007/S10482-019-01314-3

Chamas, A., Moon, H., Zheng, J., Qiu, Y., Tabassum, T., Jang, J. H., Abu-Omar, M., Scott, S. L., & Suh, S. (2020). Degradation rates of plastics in the environment. *ACS Sustainable Chemistry & Engineering*, *8*(9), 3494–3511. https://doi.org/10.1021/acssuschemeng.9b06635

Chen, M. Y., Wu, S. H., Lin, G. H., Lu, C. P., Lin, Y. T., Chang, W. C., & Tsay, S. S. (2004). *Rubrobacter taiwanensis* sp. nov., a novel thermophilic, radiation-resistant species isolated from hot springs. *International Journal of Systematic and Evolutionary Microbiology*, *54*(5), 1849–1855. https://doi.org/10.1099/IJS.0.63109-0

Chen, R. W., Li, C., He, Y. Q., Cui, L. Q., Long, L. J., & Tian, X. P. (2020). *Rubrobacter tropicus* sp. nov. and *Rubrobacter marinus* sp. nov., isolated from deep-sea sediment of the South China Sea. *International Journal of Systematic and Evolutionary Microbiology*, *70*(10), 5576-5585. https://doi.org/10.1099/ijsem.0.004449

Chen, R. W., Wang, K. X., Wang, F. Z., He, Y. Q., Long, L. J., & Tian, X. P. (2018). *Rubrobacter indicoceani* sp. nov., a new marine actinobacterium isolated from Indian Ocean sediment. *International Journal of Systematic and Evolutionary Microbiology*, *68*(11), 3487-3493. https://doi.org/10.1099/ijsem.0.003018

Cui, Y. W., Gong, X. Y., Shi, Y. P., & Wang, Z. (2017). Salinity effect on production of PHA and EPS by *Haloferax mediterranei*. *RSC Advances*, *7*(84), 53587–53595. https://doi.org/10.1039/C7RA09652F

Duvigneau, S., Kettner, A., Carius, L., Griehl, C., Findeisen, R., & Kienle, A. (2021). Fast, inexpensive, and reliable HPLC method to determine monomer fractions in

poly(3-hydroxybutyrate-co-3-hydroxyvalerate). *Applied Microbiology and Biotechnology*, *105*(11), 4743–4749. https://doi.org/10.1007/S00253-021-11265-3

Emadian, S. M., Onay, T. T., & Demirel, B. (2017). Biodegradation of bioplastics in natural environments. *Waste Management*, *59*, 526–536. https://doi.org/10.1016/J.WASMAN.2016.10.006

Fernandes, M., Salvador, A., Alves, M. M., & Vicente, A. A. (2020). Factors affecting polyhydroxyalkanoates biodegradation in soil. *Polymer Degradation and Stability*, *182*, 109408. https://doi.org/10.1016/J.POLYMDEGRADSTAB.2020.109408

Fialová, D., Skoupý, R., Drozdová, E., Paták, A., Piňos, J., Šín, L., Beňuš, R., & Klíma, B. (2017). The application of scanning electron microscopy with energy-dispersive x-ray spectroscopy (SEM-EDX) in ancient dental calculus for the reconstruction of human habits. *Microscopy and Microanalysis*, *23*(6), 1207–1213. https://doi.org/10.1017/S1431927617012661

Fredi, G., & Dorigato, A. (2021). Recycling of bioplastic waste: A review. *Advanced Industrial and Engineering Polymer Research*, *4*(3), 159–177. https://doi.org/10.1016/J.AIEPR.2021.06.006

Gallion, L. A., Anttila, M. M., Abraham, D. H., Proctor, A., & Allbritton, N. L. (2020). Preserving single cells in space and time for analytical assays. *TrAC Trends in Analytical Chemistry*, *122*, 115723. https://doi.org/10.1016/J.TRAC.2019.115723

Giedraitytė, G., & Kalėdienė, L. (2015). Purification and characterization of polyhydroxybutyrate produced from thermophilic *Geobacillus* sp. AY 946034 strain. *Chemija*, *26*(1), 38–45.

Govindasamy, S., Syafiq, I. M., Amirul, A. A. A., Amin, R. M., & Bhubalan, K. (2019). Dataset on controlled production of polyhydroxyalkanoate-based microbead using double emulsion solvent evaporation technique. *Data in Brief*, *23*, 103675. https://doi.org/10.1016/J.DIB.2019.01.023

Gupta, J., Rathour, R., Maheshwari, N., & Shekhar Thakur, I. (2021). Integrated analysis of Whole genome sequencing and life cycle assessment for polyhydroxyalkanoates production by *Cupriavidus* sp. ISTL7. *Bioresource Technology*, *337*, 125418. https://doi.org/10.1016/J.BIORTECH.2021.125418

Hejazi, P., Vasheghani-Farahani, E., & Yamini, Y. (2003). Supercritical Fluid Disruption of *Ralstonia eutropha* for Poly(β-hydroxybutyrate) Recovery. *Biotechnology Progress*, *19*(5), 1519–1523. https://doi.org/10.1021/BP034010Q

Helm, D., Labischinski, H., Schallehn, G., & Naumann, D. (1991). Classification and identification of bacteria by Fourier-transform infrared spectroscopy. *Journal of General Microbiology*, *137*(1), 69–79. https://doi.org/10.1099/00221287-137-1-69

Huschner, F., Grousseau, E., Brigham, C. J., Plassmeier, J., Popovic, M., Rha, C., & Sinskey, A. J. (2015). Development of a feeding strategy for high cell and PHA density fed-batch fermentation of *Ralstonia eutropha* H16 from organic acids and their salts. *Process Biochemistry*, *50*(2), 165–172. https://doi.org/10.1016/J.PROCBIO.2014.12.004

Ibrahim, N. I., Shahar, F. S., Hameed Sultan, M. T., Md Shah, A. U., Azrie Safri, S. N., & Mat Yazik, M. H. (2021). Overview of Bioplastic Introduction and Its Applications in Product Packaging. *Coatings 2021*, *11*(11), 1423. https://doi.org/10.3390/COATINGS11111423

Jendrossek, D. (2009). Polyhydroxyalkanoate granules are complex subcellular organelles (carbonosomes). *Journal of bacteriology*, *191*(10), 3195-3202. https://doi.org/10.1128/jb.01723-08

Jendrossek, D., Schirmer, A., & Schlegel, H. G. (1996). Biodegradation of polyhydroxyalkanoic acids. *Applied Microbiology and Biotechnology*, *46*(5–6), 451–463. https://doi.org/10.1007/S002530050844

Jia, K., Cao, R., Hua, D. H., & Li, P. (2016). Study of Class I and Class III Polyhydroxyalkanoate (PHA) Synthases with Substrates Containing a Modified Side Chain. *Biomacromolecules*, *17*(4), 1477. https://doi.org/10.1021/ACS.BIOMAC.6B00082

Jian, J., Xiangbin, Z., & Xianbo, H. (2020). An overview on synthesis, properties and applications of poly(butylene-adipate-co-terephthalate)–PBAT. *Advanced Industrial and Engineering Polymer Research*, *3*(1), 19–26. https://doi.org/10.1016/J.AIEPR.2020.01.001

Jurado, V., Miller, A. Z., Alias-Villegas, C., Laiz, L., & Saiz-Jimenez, C. (2012). *Rubrobacter bracarensis* sp. nov., a novel member of the genus *Rubrobacter* isolated from a biodeteriorated monument. *Systematic and Applied Microbiology*, *35*(5), 306–309. https://doi.org/10.1016/J.SYAPM.2012.04.007

Kämpfer, P., Glaeser, S. P., Busse, H. J., Abdelmohsen, U. R., & Hentschel, U. (2014). *Rubrobacter aplysinae* sp. nov., isolated from the marine sponge *Aplysina aerophoba*. *International Journal of Systematic and Evolutionary Microbiology*, *64*(PART 3), 705–709. https://doi.org/10.1099/IJS.0.055152-0

Kaniuk, Ł., & Stachewicz, U. (2021). Development and advantages of biodegradable PHA polymers based on electrospun PHBV fibers for tissue engineering and other biomedical applications. *ACS Biomaterials Science and Engineering*, *7*(12), 5339–5362. https://doi.org/10.1021/ACSBIOMATERIALS.1C00757

Karasavvas, E., & Chatzidoukas, C. (2020). Model-based dynamic optimization of the fermentative production of polyhydroxyalkanoates (PHAs) in fed-batch and sequence of continuously operating bioreactors. *Biochemical Engineering Journal*, *162*, 107702. https://doi.org/10.1016/J.BEJ.2020.107702

Kasavan, S., Yusoff, S., Rahmat Fakri, M. F., & Siron, R. (2021). Plastic pollution in water ecosystems: A bibliometric analysis from 2000 to 2020. *Journal of Cleaner Production*, *313*, 127946. https://doi.org/10.1016/J.JCLEPRO.2021.127946

Kessler, B., & Witholt, B. (2001). Factors involved in the regulatory network of polyhydroxyalkanoate metabolism. *Journal of biotechnology*, *86*(2), 97-104. https://doi.org/10.1016/S0168-1656(00)00404-1

Khanna, S., & Srivastava, A. K. (2005). Recent advances in microbial polyhydroxyalkanoates. *Process Biochemistry*, *40*(2), 607–619. https://doi.org/10.1016/J.PROCBIO.2004.01.053

Kichise, T., Taguchi, S., & Doi, Y. (2002). Enhanced accumulation and changed monomer composition in polyhydroxyalkanoate (PHA) copolyester by in vitro evolution of *Aeromonas caviae* PHA synthase. *Applied and Environmental Microbiology*, *68*(5), 2411–2419. https://doi.org/10.1128/AEM.68.5.2411-2419.2002

King B. (2023). *Why are BP, Shell, and other oil giants making so much money right now? - BBC News*. Retrieved June 16, 2023, from https://www.bbc.com/news/business-64583982

Kjeldsen, A., Price, M., Lilley, C., Guzniczak, E., & Archer, I. (2018). A review of standards for biodegradable plastics. *Industrial Biotechnology Innovation Centre*, *33*(1).

Koller, M. (2017). Production of Poly Hydroxyalkanoate (PHA) biopolyesters by extremophiles. *MOJ Polymer Science*, *Volume 1*(Issue 2). https://doi.org/10.15406/MOJPS.2017.01.00011

Koller, M. (2018). A review on established and emerging fermentation schemes for microbial production of polyhydroxyalkanoate (PHA) biopolyesters. *Fermentation 2018*, *4*(2), 30. https://doi.org/10.3390/FERMENTATION4020030

Koller, M., & Braunegg, G. (2015). Potential and prospects of continuous polyhydroxyalkanoate (PHA) production. *Bioengineering*, *2*(2), 94–121. https://doi.org/10.3390/BIOENGINEERING2020094

Koller, M., Niebelschütz, H., & Braunegg, G. (2013). Strategies for recovery and purification of poly[(R)-3-hydroxyalkanoates] (PHA) biopolyesters from surrounding biomass. *Engineering in Life Sciences*, *13*(6), 549–562. https://doi.org/10.1002/ELSC.201300021

Kouřilová, X., Schwarzerová, J., Pernicová, I., Sedlář, K., Mrázová, K., Krzyžánek, V., Nebesářová, J., & Obruča, S. (2021). the first insight into polyhydroxyalkanoates accumulation in multi-extremophilic *Rubrobacter xylanophilus* and *Rubrobacter spartanus*. *Microorganisms*, *9*(5). https://doi.org/10.3390/MICROORGANISMS9050909

Kumar, P., & Kim, B. S. (2018). Valorization of polyhydroxyalkanoates production process by co-synthesis of value-added products. *Bioresource technology*, *269*, 544-556. https://doi.org/10.1016/j.biortech.2018.08.120

Lai, J., Huang, H., Lin, M., Xu, Y., Li, X., & Sun, B. (2023). Enzyme catalyzes ester bond synthesis and hydrolysis: The key step for sustainable usage of plastics. *Frontiers in Microbiology*, *13*, 1113705. https://doi.org/10.3389/fmicb.2022.1113705

Law, J. H., & Slepecky, R. A. (1961). Assay of poly-β-hydroxybutyric acid. *Journal of bacteriology*, *82*(1), 33-36. https://doi.org/10.1128/JB.82.1.37-42.1961

Lee, S. Y., Lee, Y. K., & Chang, H. N. (1995). Stimulatory effects of amino acids and oleic acid on poly(3-hydroxybutyric acid) synthesis by recombinant *Escherichia coli*. *Journal of Fermentation and Bioengineering*, *79*(2), 177–180. https://doi.org/10.1016/0922-338X(95)94089-A

Legat, A., Gruber, C., Zangger, K., Wanner, G., & Stan-Lotter, H. (2010). Identification of polyhydroxyalkanoates in *Halococcus* and other haloarchaeal species. *Applied Microbiology and Biotechnology*, *87*, 1119-1127. https://doi.org/10.1007/s00253-010-2611-6

Lenz, R. W., & Marchessault, R. H. (2004). Bacterial polyesters: biosynthesis, biodegradable plastics and biotechnology. *Biomacromolecules*, *6*(1), 1–8. https://doi.org/10.1021/BM049700C

Liu, M., González, J. E., Willis, L. B., & Walker, G. C. (1998). A novel screening method for isolating exopolysaccharide-deficient mutants. *Applied and Environmental Microbiology*, *64*(11), 4600. https://doi.org/10.1128/AEM.64.11.4600-4602.1998

López-Abelairas, M., García-Torreiro, M., Lú-Chau, T., Lema, J. M., & Steinbüchel, A. (2015). Comparison of several methods for the separation of poly(3-hydroxybutyrate) from *Cupriavidus necator* H16 cultures. *Biochemical Engineering Journal*, *93*, 250–259. https://doi.org/10.1016/J.BEJ.2014.10.018

Marasco, R., Michoud, G., Sefrji, F. O., Fusi, M., Antony, C. P., Seferji, K. A., Barozzi, A., Merlino, G., & Daffonchio, D. (2023). The identification of the new species *Nitratireductor thuwali* sp. nov. reveals the untapped diversity of hydrocarbon-degrading culturable bacteria from the arid mangrove sediments of the Red Sea. *Frontiers in Microbiology*, *14*, 1155381. https://doi.org/10.3389/FMICB.2023.1155381

Mascarenhas, J., & Aruna, K. (2017). Screening of polyhydroxyalkonates (PHA) accumulating bacteria from diverse habitats. *Journal of Global Biosciences*, 6(3), 4835-4848. https://doi.org/10.13140/RG.2.2.29966.72005

Meereboer, K. W., Misra, M., & Mohanty, A. K. (2020). Review of recent advances in the biodegradability of polyhydroxyalkanoate (PHA) bioplastics and their composites. *Green Chemistry*, *22*(17), 5519–5558. https://doi.org/10.1039/D0GC01647K

Meng, D. C., Shen, R., Yao, H., Chen, J. C., Wu, Q., & Chen, G. Q. (2014). Engineering the diversity of polyesters. *Current Opinion in Biotechnology*, *29*(1), 24–33. https://doi.org/10.1016/J.COPBIO.2014.02.013

Mesquita, D. P., Amaral, A. L., Leal, C., Oehmen, A., Reis, M. A. M., & Ferreira, E. C. (2015). Polyhydroxyalkanoate granules quantification in mixed microbial cultures using image analysis: Sudan Black B versus Nile Blue A staining. *Analytica Chimica Acta*, *865*(1), 8–15. https://doi.org/10.1016/J.ACA.2015.01.018

Mohanrasu, K., Guru Raj Rao, R., Dinesh, G. H., Zhang, K., Sudhakar, M., Pugazhendhi, A., Jeyakanthan, J., Ponnuchamy, K., Govarthanan, M., & Arun, A. (2021). Production and characterization of biodegradable polyhydroxybutyrate by

Micrococcus luteus isolated from marine environment. *International Journal of Biological Macromolecules*, *186*, 125–134. https://doi.org/10.1016/J.IJBIOMAC.2021.07.029

Możejko-Ciesielska, J., & Kiewisz, R. (2016). Bacterial polyhydroxyalkanoates: Still fabulous? *Microbiological Research*, *192*, 271–282. https://doi.org/10.1016/J.MICRES.2016.07.010

Neoh, S. Z., Fey Chek, M., Tiang Tan, H., Linares-Pastén, J. A., Nandakumar, A., Hakoshima, T., & Sudesh, K. (2022). Polyhydroxyalkanoate synthase (PhaC): The key enzyme for biopolyester synthesis. *Current Research in Biotechnology*, *4*, 87–101. https://doi.org/10.1016/J.CRBIOT.2022.01.002

Norman, J. S., King, G. M., & Friesen, M. L. (2017). *Rubrobacter spartanus* sp. nov., a moderately thermophilic oligotrophic bacterium isolated from volcanic soil. *International journal of systematic and evolutionary microbiology*, *67*(9), 3597-3602. https://doi.org/10.1099/ijsem.0.002175

Novais, Â., & Peixe, L. (2021). Fourier transform infrared spectroscopy (FT-IR) for food and water microbiology. *Application and Integration of Omics-Powered Diagnostics in Clinical and Public Health Microbiology*, 191–217. https://doi.org/10.1007/978-3-030-62155-1_11

Nwinyi, O. C., & Owolabi, T. A. (2019). Scanning electron microscopy and Fourier transmission analysis of polyhydroxyalkanoates isolated from bacteria species from abattoir in Ota, Nigeria. *Journal of King Saud University - Science*, *31*(3), 285–298. https://doi.org/10.1016/J.JKSUS.2017.08.003

Obruča, S., Dvořák, P., Sedláček, P., Koller, M., Sedlář, K., Pernicová, I., & Šafránek, D. (2022). Polyhydroxyalkanoates synthesis by halophiles and thermophiles: towards sustainable production of microbial bioplastics. *Biotechnology Advances*, *58*, 107906. https://doi.org/10.1016/j.biotechadv.2022.107906

Obruča, S., Sedlacek, P., Koller, M., Kucera, D., & Pernicova, I. (2018). Involvement of polyhydroxyalkanoates in stress resistance of microbial cells: Biotechnological consequences and applications. *Biotechnology Advances*, *36*(3), 856–870. https://doi.org/10.1016/J.BIOTECHADV.2017.12.006

Obruča, S., Sedlacek, P., Mravec, F., Krzyzanek, V., Nebesarova, J., Samek, O., Kucera, D., Benesova, P., Hrubanova, K., Milerova, M., & Marova, I. (2017). The presence of PHB granules in cytoplasm protects non-halophilic bacterial cells against the harmful impact of hypertonic environments. *New Biotechnology*, *39*, 68–80. https://doi.org/10.1016/J.NBT.2017.07.008

Obruča, S., Sedlacek, P., Slaninova, E., Fritz, I., Daffert, C., Meixner, K., Sedrlova, Z., & Koller, M. (2020). Novel unexpected functions of PHA granules. *Applied Microbiology and Biotechnology 2020*, *104*(11), 4795–4810. https://doi.org/10.1007/S00253-020-10568-1

Obulisamy, P. K., & Mehariya, S. (2021). Polyhydroxyalkanoates from extremophiles: A review. *Bioresource Technology*, *325*, 124653. https://doi.org/10.1016/J.BIORTECH.2020.124653

Onour, I., & Abdo, M. M. (2022). Sensitivity of Crude Oil Price Change to Major Global Factors and to Russian-Ukraine War Crisis. *SSRN Electronic Journal*. https://doi.org/10.2139/SSRN.4187797

Oren, A., & Garrity, G. M. (2021). Valid publication of the names of forty-two phyla of prokaryotes. *International journal of systematic and evolutionary microbiology*, *71*(10), 005056. https://doi.org/10.1099/ijsem.0.005056

Oryan, A., Alidadi, S., Moshiri, A., & Maffulli, N. (2014). Bone regenerative medicine: classic options, novel strategies, and future directions. *Journal of Orthopaedic Surgery and Research 2014*, *9*(1), 1–27. https://doi.org/10.1186/1749-799X-9-18

Ostle, A. G., & Holt, J. G. (1982). Nile blue A as a fluorescent stain for poly-beta-hydroxybutyrate. *Applied and Environmental Microbiology*, *44*(1), 238–241. https://doi.org/10.1128/AEM.44.1.238-241.1982

Pagliano, G., Galletti, P., Samorì, C., Zaghini, A., & Torri, C. (2021). Recovery of polyhydroxyalkanoates from single and mixed microbial cultures: A Review. *Frontiers in Bioengineering and Biotechnology*, *9*, 54. https://doi.org/10.3389/FBIOE.2021.624021

Palmeiro-Sánchez, T., O'Flaherty, V., & Lens, P. N. L. (2022). Polyhydroxyalkanoate bio-production and its rise as biomaterial of the future. *Journal of Biotechnology*, *348*, 10–25. https://doi.org/10.1016/J.JBIOTEC.2022.03.001

Pradhan, S., Dikshit, P. K., & Moholkar, V. S. (2018). Production, ultrasonic extraction, and characterization of poly (3-hydroxybutyrate) (PHB) using *Bacillus megaterium* and *Cupriavidus necator*. *Polymers for Advanced Technologies*, *29*(8), 2392–2400. https://doi.org/10.1002/PAT.4351

Prata, J. C., Silva, A. L. P., Duarte, A. C., & Rocha-Santos, T. (2022). The road to sustainable use and waste management of plastics in Portugal. *Frontiers of Environmental Science and Engineering*, *16*(1), 1–16. https://doi.org/10.1007/S11783-021-1439-X

Prieto, A., Escapa, I. F., Martínez, V., Dinjaski, N., Herencias, C., de la Peña, F., Tarazona, N., & Revelles, O. (2016). A holistic view of polyhydroxyalkanoate metabolism in *Pseudomonas putida*. *Environmental Microbiology*, *18*(2), 341–357. https://doi.org/10.1111/1462-2920.12760

Purushothaman, M., Anderson, R. K. I., Narayana, S., & Jayaraman, V. K. (2001). Industrial byproducts as cheaper medium components influencing the production of polyhydroxyalkanoates (PHA) - Biodegradable plastics. *Bioprocess and Biosystems Engineering*, *24*(3), 131–136. https://doi.org/10.1007/S004490100240

Ramsay, J. A., Berger, E., Ramsay, B. A., & Chavarie, C. (1990). Recovery of poly-3-hydroxyalkanoic acid granules by a surfactant-hypochlorite treatment. *Biotechnology Techniques*, *4*(4), 221–226. https://doi.org/10.1007/BF00158833

Rehakova, V., Pernicova, I., Kouřilová, X., Sedlacek, P., Musilova, J., Sedlar, K., Koller, M., Kalina, M., & Obruča, S. (2023). Biosynthesis of versatile PHA copolymers by thermophilic members of the genus *Aneurinibacillus*. *International Journal of Biological Macromolecules*, *225*, 1588–1598. https://doi.org/10.1016/J.IJBIOMAC.2022.11.215

Robert, X., & Gouet, P. (2014). Deciphering key features in protein structures with the new ENDscript server. *Nucleic Acids Research*, *42*(1), 320–324. https://doi.org/10.1093/NAR/GKU316

Rodríguez-Contreras, A., Guillem-Marti, J., Lopez, O., Manero, J. M., & Ruperez, E. (2019). Antimicrobial PHAs coatings for solid and porous tantalum implants. *Colloids and Surfaces B: Biointerfaces*, *182*, 110317. https://doi.org/10.1016/J.COLSURFB.2019.06.047

Sagong, H. Y., Son, H. F., Choi, S. Y., Lee, S. Y., & Kim, K. J. (2018). Structural Insights into Polyhydroxyalkanoates Biosynthesis. *Trends in Biochemical Sciences*, *43*(10), 790–805. https://doi.org/10.1016/J.TIBS.2018.08.005

Samrot, A. V., Samanvitha, S. K., Shobana, N., Renitta, E. R., Kumar, P. S., Kumar, S. S., Abirami, S., Dhiva, S., Bavanilatha, M., Prakash, P., Saigeetha, S., Shree, K. S., & Thirumurugan, R. (2021). The Synthesis, Characterization and Applications of Polyhydroxyalkanoates (PHAs) and PHA-Based Nanoparticles. *Polymers*, *13*(19). https://doi.org/10.3390/POLYM13193302

Sangkharak, K., & Prasertsan, P. (2012). Screening and identification of polyhydroxyalkanoates producing bacteria and biochemical characterization of their possible application. *The Journal of General and Applied Microbiology*, *58*(3), 173–182. https://doi.org/10.2323/JGAM.58.173

Saponetti S., M., Bobba, F., Salerno, G., Scarfato, A., Corcelli, A., & Cucolo, A. (2011). Morphological and structural aspects of the extremely halophilic archaeon *Haloquadratum walsbyi*. *PLOS One*, *6*(4), e18653. https://doi.org/10.1371/journal.pone.0018653

Satoh, H., Sakamoto, T., Kuroki, Y., Kudo, Y., & Mino, T. (2016). Application of the Alkaline-Digestion-HPLC method to the rapid determination of polyhydroxyalkanoate in activated sludge. *Journal of Water and Environment Technology*, *14*(5), 411–421. https://doi.org/10.2965/JWET.16-027

Sayers, E. W., Cavanaugh, M., Clark, K., Ostell, J., Pruitt, K. D., & Karsch-Mizrachi, I. (2020). GenBank. *Nucleic Acids Research*, *48*(1), 84–86. https://doi.org/10.1093/NAR/GKZ956

Sedlacek, P., Slaninova, E., Enev, V., Koller, M., Nebesarova, J., Marova, I., Hrubanova K., Krzyzanek V., Samek O., & Obruča, S. (2019). What keeps polyhydroxyalkanoates in bacterial cells amorphous? A derivation from stress exposure experiments. *Applied microbiology and biotechnology*, *103*, 1905-1917. https://doi.org/10.1007/s00253-018-09584-z

Selvarajan, R., Sibanda, T., & Tekere, M. (2018). Thermophilic bacterial communities inhabiting the microbial mats of “indifferent” and chalybeate (iron-rich) thermal springs: Diversity and biotechnological analysis. *Microbiology Open*, *7*(2), e00560. https://doi.org/10.1002/MBO3.560

Shahid, S., Razzaq, S., Farooq, R., & Nazli, Z. i. H. (2021). Polyhydroxyalkanoates: Next generation natural biomolecules and a solution for the world’s future economy. *International Journal of Biological Macromolecules*, *166*, 297–321. https://doi.org/10.1016/J.IJBIOMAC.2020.10.187

Shamsuddin M., I. M., Ahmad Jafar, J. A., Sadiq Abdulrahman Shawai, A. S. A., Yusuf, S., Lateefah, M., & Aminu, I. (2017). Bioplastics as better alternative to petroplastics and their role in national sustainability: A Review. *Advances in Bioscience and Bioengineering*, *5*(4), 63. https://doi.org/10.11648/J.ABB.20170504.13

Simó-Cabrera, L., García-Chumillas, S., Hagagy, N., Saddiq, A., Tag, H., Selim, S., Abdelgawad, H., Agüero, A. A., Sánchez, F. M., Cánovas, V., Pire, C., & Martínez-Espinosa, R. M. (2021). Haloarchaea as cell factories to produce bioplastics. *Marine Drugs*, *19*(3). https://doi.org/10.3390/MD19030159

Singh, M. K., Rai, P. K., Rai, A., Singh, S., & Singh, J. S. (2019). Poly-β-hydroxybutyrate production by the cyanobacterium *scytonema geitleri* bharadwaja under varying environmental conditions. *Biomolecules 2019*, *9*(5), 198. https://doi.org/10.3390/BIOM9050198

Siracusa, V., & Blanco, I. (2020). Bio-Polyethylene (Bio-PE), Bio-Polypropylene (Bio-PP) and Bio-Poly(ethylene terephthalate) (Bio-PET): Recent developments in bio-based polymers analogous to petroleum-derived ones for packaging and engineering applications. *Polymers*, *12*(8), 1641. https://doi.org/10.3390/POLYM12081641

Sruamsiri, D., Thayanukul, P., & Suwannasilp, B. B. (2020). In situ identification of polyhydroxyalkanoate (PHA)-accumulating microorganisms in mixed microbial cultures under feast/famine conditions. *Scientific Reports 2020*, *10*(1), 1–10. https://doi.org/10.1038/s41598-020-60727-7

Stanley, A., Punil Kumar, H. N., Mutturi, S., & Vijayendra, S. V. N. (2018). Fed-Batch Strategies for Production of PHA Using a Native Isolate of *Halomonas venusta* KT832796 Strain. *Applied Biochemistry and Biotechnology*, *184*(3), 935–952. https://doi.org/10.1007/S12010-017-2601-6

Steinbüchel, A., & Schlegel, H. G. (1991). Physiology and molecular genetics of poly(β-hydroxyalkanoic acid) synthesis in *Alcaligenes eutrophus*. *Molecular Microbiology*, *5*(3), 535–542. https://doi.org/10.1111/J.1365-2958.1991.TB00725.X

Suzuki, K., Collins, M. D., Iijima, E., & Komagata, K. (1988). Chemotaxonomic characterization of a radiotolerant bacterium, *Arthrobacter radiotolerans*: Description of *Rubrobacter radiotolerans* gen. nov., comb. nov. *FEMS Microbiology Letters*, *52*(1–2), 33–39. https://doi.org/10.1111/J.1574-6968.1988.TB02568.X

Tamura, K., Stecher, G., & Kumar, S. (2021). MEGA11: Molecular Evolutionary Genetics Analysis Version 11. *Molecular Biology and Evolution*, *38*(7), 3022–3027. https://doi.org/10.1093/MOLBEV/MSAB120

Tan, D., Yin, J., & Chen, G. Q. (2017). Production of polyhydroxyalkanoates. *In Current developments in biotechnology and bioengineering* (655-692). https://doi.org/10.1016/B978-0-444-63662-1.00029-4

Tan, G. Y. A., Chen, C. L., Li, L., Ge, L., Wang, L., Razaad, I. M. N., Li, Y., Zhao, L., Mo, Y., & Wang, J. Y. (2014). Start a research on biopolymer polyhydroxyalkanoate (PHA): a review. *Polymers*, *6*(3), 706-754. https://doi.org/10.3390/POLYM6030706

Thakur, S., Chaudhary, J., Sharma, B., Verma, A., Tamulevicius, S., & Thakur, V. K. (2018). Sustainability of bioplastics: Opportunities and challenges. *Current Opinion in Green and Sustainable Chemistry*, *13*, 68–75. https://doi.org/10.1016/J.COGSC.2018.04.013

Thomas, T., Sudesh, K., Bazire, A., Elain, A., Tan, H. T., Lim, H., & Bruzaud, S. (2020). PHA Production and PHA Synthases of the Halophilic Bacterium *Halomonas* sp. SF2003. *Bioengineering 2020*, *7*(1), 29. https://doi.org/10.3390/BIOENGINEERING7010029

Tokiwa, Y., Calabia, B. P., Ugwu, C. U., & Aiba, S. (2009). Biodegradability of Plastics. *International Journal of Molecular Sciences 2009*, *10*(9), 3722–3742. https://doi.org/10.3390/IJMS10093722

Tsuge, T., Hyakutake, M., & Mizuno, K. (2015). Class IV polyhydroxyalkanoate (PHA) synthases and PHA-producing Bacillus. *Applied Microbiology and Biotechnology*, *99*(15), 6231–6240. https://doi.org/10.1007/S00253-015-6777-9

Urbieta, M. S., Donati, E. R., Chan, K. G., Shahar, S., Sin, L. L., & Goh, K. M. (2015). Thermophiles in the genomic era: Biodiversity, science, and applications. *Biotechnology Advances*, *33*(6), 633-647. https://doi.org/10.1016/j.biotechadv.2015.04.007

Vicente, D., Proença, D. N., & Morais, P. V. (2023). The Role of Bacterial Polyhydroalkanoate (PHA) in a Sustainable Future: A Review on the Biological Diversity. *International Journal of Environmental Research and Public Health 2023*, *20*(4), 2959. https://doi.org/10.3390/IJERPH20042959

Wang, F., & Lee, S. Y. (1997). Poly(3-Hydroxybutyrate) Production with High Productivity and High Polymer Content by a Fed-Batch Culture of Alcaligenes latus under Nitrogen Limitation. *Applied and Environmental Microbiology*, *63*(9), 3703–3706. https://doi.org/10.1128/AEM.63.9.3703-3706.1997

Wang, Q., Yu, H., Xia, Y., Kang, Z., & Qi, Q. (2009). Complete PHB mobilization in *Escherichia coli* enhances the stress tolerance: A potential biotechnological application. *Microbial Cell Factories*, *8*(1), 47. https://doi.org/10.1186/1475-2859-8-47

Wang, S., Chen, W., Xiang, H., Yang, J., Zhou, Z., & Zhu, M. (2016). Modification and Potential Application of Short-Chain-Length Polyhydroxyalkanoate (SCL-PHA). *Polymers 2016*, *8*(8), 273. https://doi.org/10.3390/POLYM8080273

Watanabe, Y., Ichinomiya, Y., Shimada, D., Saika, A., Abe, H., Taguchi, S., & Tsuge, T. (2012). Development and validation of an HPLC-based screening method to acquire polyhydroxyalkanoate synthase mutants with altered substrate specificity. *Journal of Bioscience and Bioengineering*, *113*(3), 286–292. https://doi.org/10.1016/J.JBIOSC.2011.10.015

Wei, Y. H., Chen, W. C., Huang, C. K., Wu, H. S., Sun, Y. M., Lo, C. W., & Janarthanan, O. M. (2011). Screening and evaluation of polyhydroxybutyrate-producing strains from indigenous isolate *Cupriavidus taiwanensis* strains. *International Journal of Molecular Sciences*, *12*(1), 252–265. https://doi.org/10.3390/IJMS12010252

Williams, S. F., Martin, D. P., Horowitz, D. M., & Peoples, O. P. (1999). PHA applications: addressing the price performance issue: I. Tissue engineering. *International Journal of Biological Macromolecules*, *25*(1–3), 111–121. https://doi.org/10.1016/S0141-8130(99)00022-7

Williamson, D. H., & Wilkinson, J. F. (1958). The isolation and estimation of the poly-beta-hydroxybutyrate inclusions of *Bacillus* species. *Journal of General Microbiology*, *19*(1), 198–209. https://doi.org/10.1099/00221287-19-1-198

Yamanè, T., & Shimizu, S. (1984). Fed-batch techniques in microbial processes. *Bioprocess Parameter Control*, 147–194. https://doi.org/10.1007/BFB0006382

Yoshinaka, T., Yano, K., & Yamaguchi, H. (1973). Isolation of highly radioresistant bacterium, *Arthrobacter radiotolerans* nov. sp. *Agricultural and Biological Chemistry*, *37*(10), 2269-2275. https://doi.org/10.1080/00021369.1973.10861003

ZEISS. (2023). *Microscopy Today*, *31*(S1), 26–26. https://doi.org/10.1093/MICTOD/QAAD007.023

7. Annexes

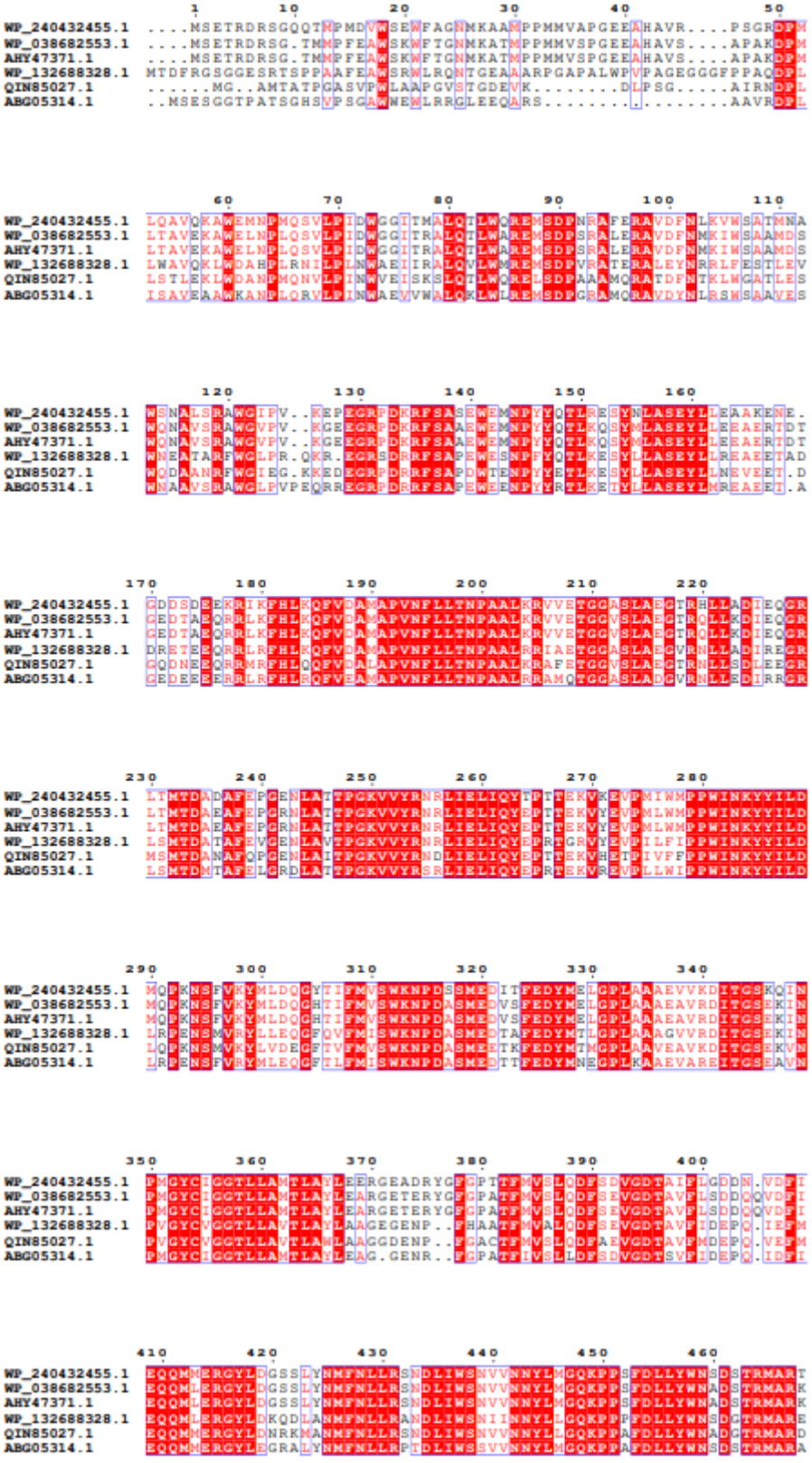
WP_240432455.1
WP_038682553.1
AHY47371.1
WP_132688328.1
QIN85027.1
ABG05314.1

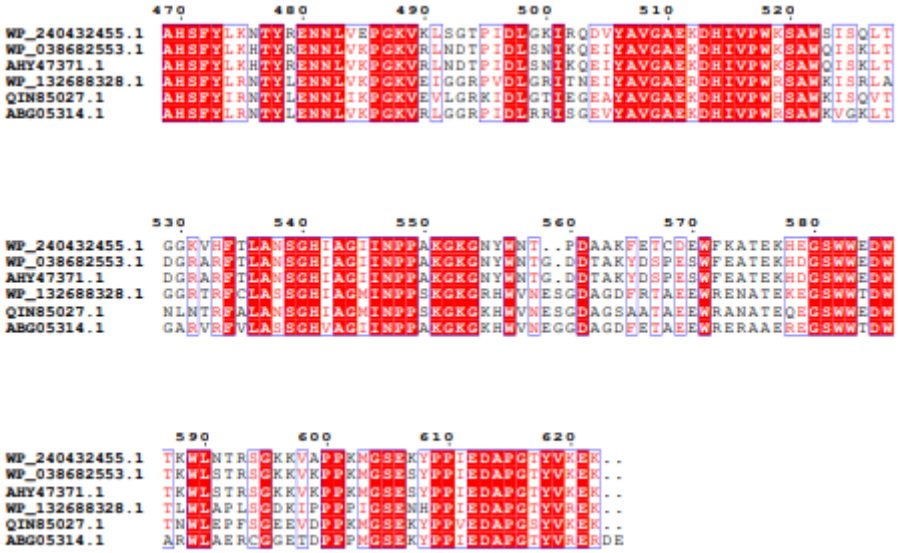

Figure 7.1. - Full sequence alignment of the *phaC* encoded protein class I

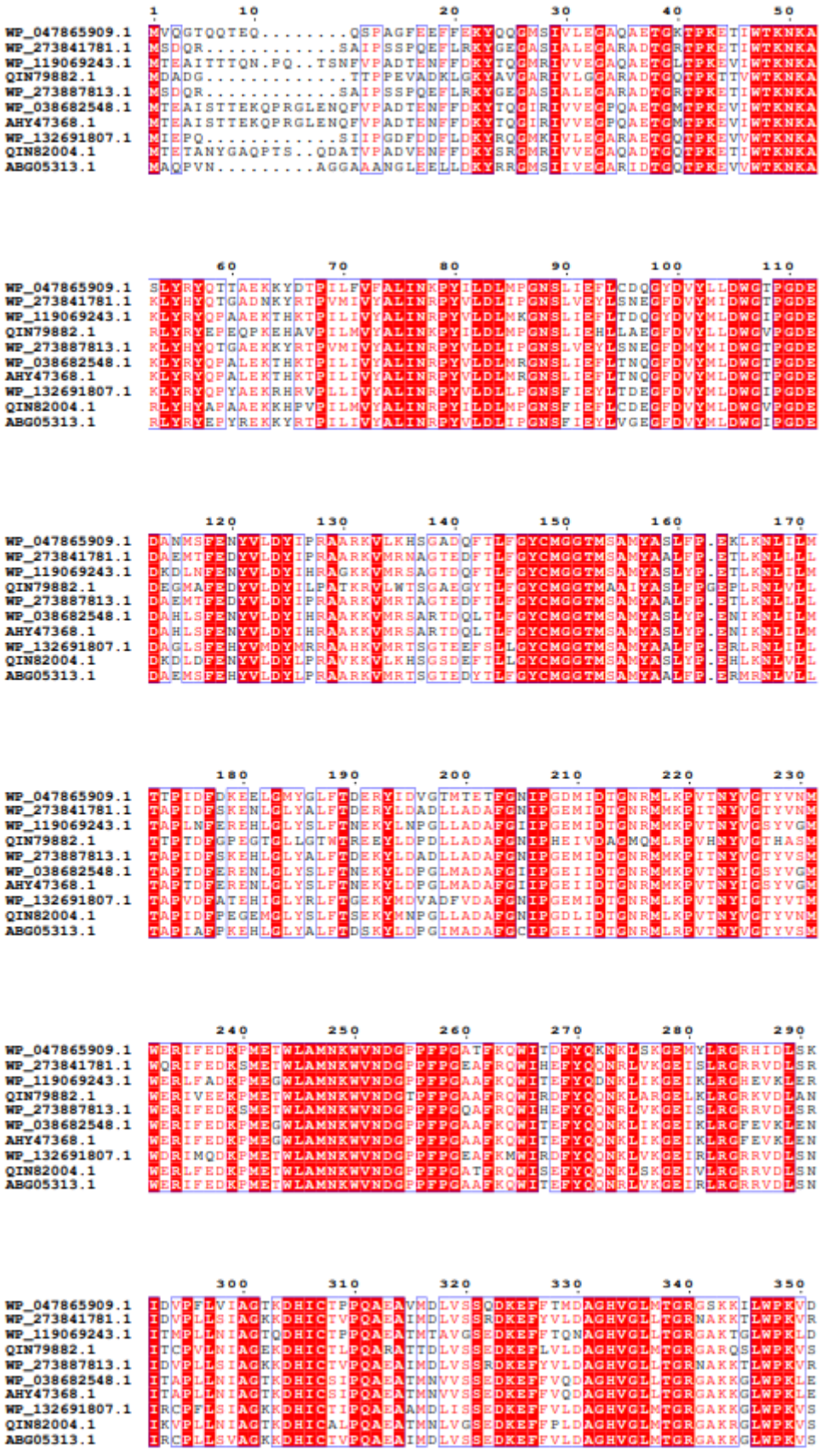
WP_047865909.1
WP_273841781.1
WP_119069243.1
QIN79882.1
WP_273887813.1
WP_038682548.1
AHY47368.1
WP_132691807.1
QIN82004.1
ABG05313.1

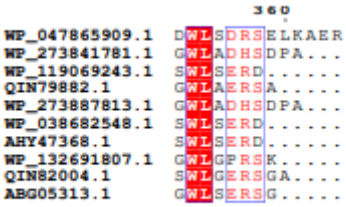

Figure 7.2. - Full sequence alignment of the *phaC* encoded protein class III